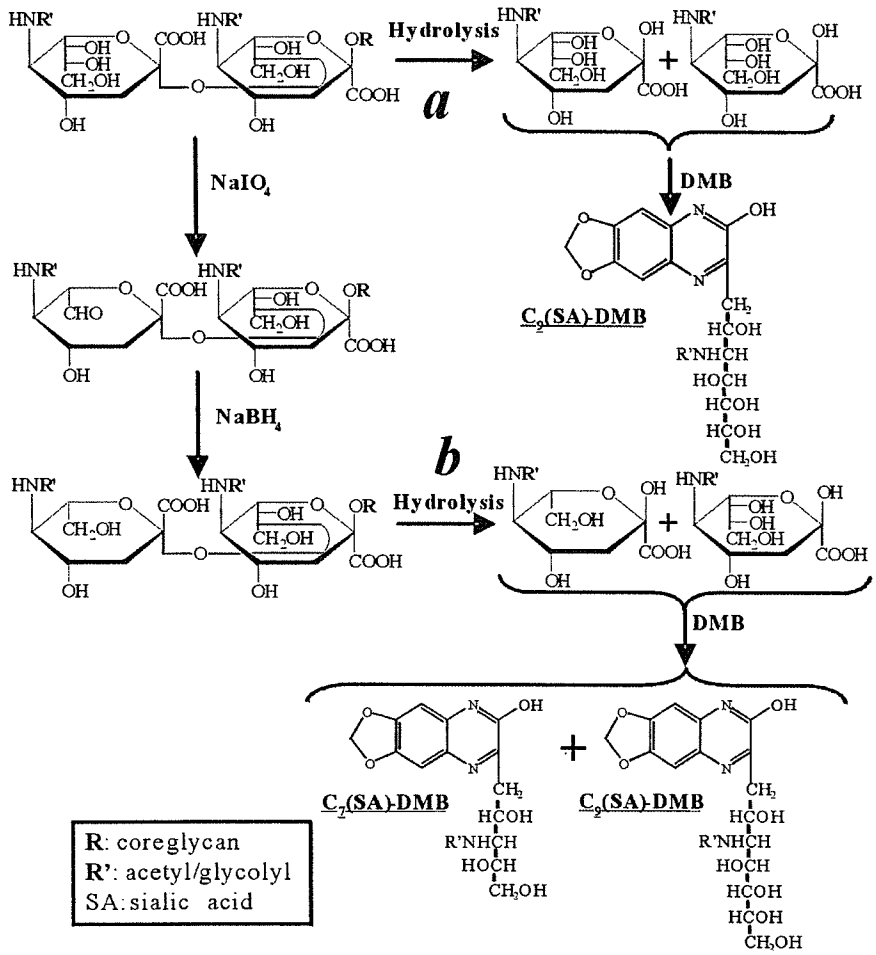

Fig. 6. Principle to detect disialyl residues in bovine AGP. Direct acid hydrolysis allows determination of compositions of sialic acids (route *a*). By hydrolysis after oxidation with periodate, the outermost sialic acids produce C-7 analogs. On the contrary, the inner sialic acids are not oxidized with periodate, and produce intact sialic acids (route *b*).

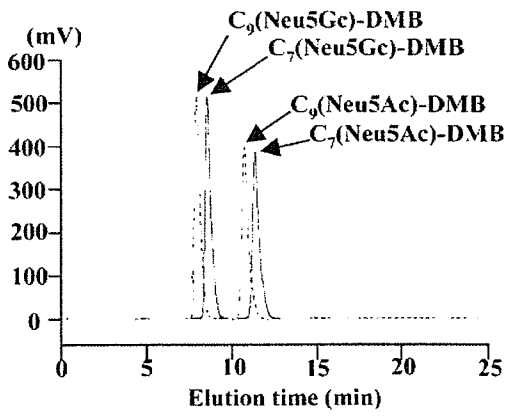

Fig. 7. Detection of disialyl residues in bovine AGP. The dotted line is a chromatogram after direct hydrolysis of bovine AGP. The solid line is a chromatogram after periodate oxidation treatment followed by hydrolysis.

Discussion

Except for human AGP, animal AGPs have received little or no attention with regard to their glycans. We analyzed oligosaccharides of AGP samples from human, bovine, sheep, and rat and compared their patterns after labeling with 2AA (Anumula and Dhume, 1998). The fluorescently labeled sialic acid–containing oligosaccharides were superbly resolved based on the number of sialic acids, and isomers of oligosaccharides having sialic acids in different positions were also resolved. In combination with MALDI-TOF MS measurement, we could identify the structures of sialo-oligosaccharides after collection of the peaks, albeit the positions where sialic acids were attached were not determined.

AGP samples from human, bovine, sheep, and rat sera manifested quite different sialo-oligosaccharides patterns. Human AGP contained di-, tri-, and tetraantennary oligosaccharides, and some of the tri- and tetraantennary oligosaccharides included a fucose residue to form sialyl

Lewis x structures, as reported previously (Sei *et al.*, 2002; Stubbs *et al.*, 1997). Rat AGP contained diantennary oligosaccharides as major oligosaccharides. An extremely complex pattern of the chromatogram indicates that rat AGP contains highly acylated oligosaccharides as also shown from MALDI-TOF MS measurement of the major peaks. On the contrary, bovine AGP contained sialo-diantennary oligosaccharides almost exclusively. Furthermore compositions of sialic acids were quite unique, and novel diantennary chains having two NeuGc residues as well as two NeuAc and both NeuAc and NeuGc residues were found abundantly. In addition, we found hypersialylated diantennary oligosaccharides that contained three or four NeuAc and NeuGc residues in various ratios.

We eliminated the possibility of the presence of disialyl linkages by two different approaches using partial acid hydrolysis and periodate oxidation. The results indicate that each sialic acid is attached to different positions (i.e., Gal residues of nonreducing termini and GlcNAc residues of Gal-GlcNAc branches). To the best of our knowledge, there have been no reports on sialyl transferase regulating biosynthesis of such hypersialylated oligosaccharides, and further studies on their biosynthesis will be required.

Regulation of NeuGc biosynthesis is known in developing pig small intestine (Malykh *et al.*, 2003). Sialic acids in bovine fetal and adult tissues were analyzed, and NeuGc was abundantly present in all bovine tissues (Schauer *et al.*, 1991). In bovine fetuin, oligosaccharides containing only NeuAc were present almost exclusively as shown in the present data (see Figure 2). We also found that NeuGc was present in various digestive organs of mice and rats in different ratios to NeuAc (Morimoto *et al.*, 2001). There are also many reports on adult animals having a higher proportion of NeuGc than young animals. AGP and fetuin are produced in liver. At fetal and newborn stages, fetuin is abundantly present in bovine sera. However, AGP is one of the major acidic proteins at adult stages in mammals, and fetuin is hardly detected. Establishment of the relationship between fetal fetuin and AGP in adult stage will be a challenging target for understanding biological regulation of these proteins and their carbohydrate chains.

Materials and methods

Materials

Bovine fetuin was obtained from Gibco (Invitrogene, Nihon-bashi, Chuo-ku, Tokyo). AGP samples of human, bovine, sheep, and rat were from Sigma (St. Louis, MO). NeuGc, α-chymotrypsin, and bicine were also purchased from Sigma. TPCK-treated trypsin was from Worthington (Lakewood, NJ). Sephadex LH-20 was from Amersham Bioscience (Uppsala, Sweden). 2AA and sodium cyanoborohydride for fluorescent labeling of oligosaccharides were from Tokyo Kasei (Chuo-ku, Tokyo). Peptide-N^4-(acetyl-β-D-glucosaminyl)asparagine amidase (*N*-glycoamidase F, E.C. 3.2.2.18) was from Roche Molecular Biochemicals (Minato-ku, Tokyo). NeuAc was donated by Drs. Tsukada and Ohta (Marukin-Bio, Uji, Kyoto, Japan). Water purified with a Milli-Q purification system (Millipore, Shinagawa-ku, Tokyo) after double distillation of deionized water was used for preparation of the eluent for HPLC. Other reagents were of the highest grade commercially available.

Analysis of carbohydrate chains released from AGP samples with N-glycoamidase F

Carbohydrate chains were released from the protein after digesting with a mixture of trypsin and chymotrypsin as reported recently (Nakano *et al.*, 2003). Briefly, a sample of AGP from animal sera (500 μg) was dissolved in 20 mM bicine buffer (pH 8.0, 50 μl) and the solution was kept at 100°C for 10 min. After cooling, trypsin (5 μg) in bicine buffer (5 μl) and chymotrypsin (5 μg) in the same buffer (5 μl) were added to the mixture, and the mixture was incubated at 37°C overnight. After the mixture was kept on a boiling water bath for 10 min, *N*-glycoamidase F (0.5 U, 1 μl) was added to the mixture and kept at 37°C for 8 h, and the mixture was again kept on a boiling water bath for 10 min.

Carbohydrate chains in the mixture thus obtained were directly labeled with 2AA according to the method reported previously (Anumula and Dhume, 1998). To the enzyme reaction mixture, was added a solution (200 μl) of 2AA and sodium cyanoborohydride, freshly prepared by dissolution of both compounds (30 mg each) in methanol (1 ml) containing 4% sodium acetate and 2% boric acid. The mixture was kept at 80°C for 1 h. After cooling, the solution was applied to a column of Sephadex LH-20 (1 × 30 cm) equilibrated with 50% aqueous methanol. Earlier eluting fractions showing fluorescence at 410 nm with irradiating at 335-nm light were collected and evaporated to dryness. The residue was dissolved in water (100 μl), a portion (10 μl) was analyzed by HPLC, and the peaks were collected for MS measurement.

HPLC of the fluorescent labeled carbohydrate chains

HPLC was performed with a Jasco apparatus equipped with two PU-980 pumps and a Jasco FP-920 fluorescence detector. Separation was done at 50°C with a polymer-based Asahi Shodex NH2P-50 4E column (Showa Denko, Tokyo; 4.6 × 250 mm) using a linear gradient formed by 2% acetic acid in acetonitrile (solvent A) and 5% acetic acid in water containing 3% triethylamine (solvent B). The column was initially equilibrated and eluted with 70% solvent A for 2 min, at which point solvent B was increased to 95% over 80 min and kept at this composition for further 100 min. The flow rate was 1.0 ml/min throughout the analysis. Detection was performed by fluorometry with $\lambda_{ex} = 350$ nm and $\lambda_{em} = 425$ nm.

MALDI-TOF MS

MALDI-TOF mass spectra of AGP samples and the fluorescent labeled oligosaccharides were measured on a Voyager DE-PRO apparatus (PE Biosystems, Framingham, MA). A nitrogen laser was used to irradiate samples at 337 nm, and an average of 50 shots was taken. The instrument was operated in linear mode using positive polarity for proteins and negative polarity for oligosaccharides, respectively, at an accelerating voltage of 20 kV. Samples (~10 pmol, 0.5 μl each) were applied to a polished stainless

steel target, to which was added a solution (0.5 μl) of 2,5-dihydroxybenzoic acid in a mixture of methanol–water (1:1). The mixture was dried in atmosphere by keeping it at room temperature for several minutes.

Detection of oligosialyl units

Bovine AGP or a fluorescent labeled oligosaccharide collected by HPLC was dried and hydrolyzed in 0.01 N TFA (20 μl) at 50°C for 1 h to release disialyl unit, and the solution was directly derivatized with DMB (Dojin) (Morimoto *et al.*, 2001; Sato *et al.*, 1999). In brief, to the hydrolyzed solution was added 100 μl of 7 mM DMB solution containing 5.0 mM TFA, 1 M 2-mercaptoetanol and 18 mM sodium hydrosulfite. The mixture was incubated at 50°C for 2 h. In the similar manner, Neu5Ac, Neu5Gc, and Neu5Acα2-8Neu5Ac (donated by Drs. Tsukada and Ohta of Marukin-Bio, Kyoto) were derivatized with DMB and used as the standard samples. A portion of the reaction mixture was analyzed on an octadecyl silica column (YMC-Pack ODS-A, 4.6 mm ID, 150 mm length, YMC Co., Kyoto, Japan) using a Shimadzu SLC10A HPLC apparatus with a Jasco FP-920 fluorometer at λ_{em} 448 nm and λ_{ex} 373 nm. The elution was performed in isocratic mode using a mixture of methanol-acetonitrile-water (14:2:84, v/v) at a flow rate of 0.9 ml/min at 40°C. At this condition, NeuAc, NeuGc, and Neu5Acα2-8Neu5Ac were observed at 10.5 min, 7.7 min, and 9.0 min, respectively.

Another approach to detect disialyl residues was performed according to the method reported by Sato *et al.* Briefly, an aqueous solution (10 μl) of bovine AGP (200 μg) was mixed with 50 mM sodium metaperiodata in 50 mM actate buffer (pH 5.0, 10 μl), and the mixture was kept at room temperature for 10 min in the dark. After addition of an aqueous solution of 10% ethyleglycol (10 μl) followed by incubation of the mixture for further 15 min at room temperature. 1 M sodium borohydride in saturated sodium bicarbonate solution (10 μl) was added to the mixture and kept at room temperature for 15 min. To remove the reagents, the reaction mixture was diluted with 300 μl water and filtered through an ultrafiltration tube (molecular cutoff 10,000; Millipore). After washing the retentate with water three times, the retentate was collected with 10 mM TFA (40 μl) and was kept for 1 h at 80°C to release sialic acids by hydrolysis. A portion (20 μl) of the mixture was derivatized with DMB and analyzed by HPLC in the same manner as described.

Abbreviations

2AA, 2-aminobenzoic acid; AGP, α1-acid glycoprotein; DMB, 1,2-diamino-4,5-methylenedioxybenzene; HPLC, high-performance liquid chromatography; MALDI-TOF MS, matrix-assisted laser-desorption/ionization time-of-flight mass spectrometry; TFA, trifluoroacetic acid.

References

Anumula, K.R. and Dhume, S.T. (1998) High resolution and high sensitivity methods for oligosaccharide mapping and characterization by normal phase high performance liquid chromatography following derivatization with highly fluorescent anthranilic acid. *Glycobiology*, **8**, 685–694.

De Graaf, T.W., Van der Stelt, M.E., Anbergen, M.G., and van Dijk, W. (1993) Inflammation-induced expression of sialyl Lewis X-containing glycan structures on alpha1-acid glycoprotein (orosomucoid) in human sera. *J. Exp. Med.*, **177**, 657–666.

Elliott, M.A., Elliott, H.G., Gallagher, K., McGuire, J., Field, M., and Smith, K.D. (1997) Investigation into the concanavalin A reactivity, fucosylation and oligosaccharide microheterogeneity of alpha1-acid glycoprotein expressed in the sera of patients with rheumatoid arthritis. *J. Chromatogr. B*, **688**, 229–237.

Fournet, B., Montreuil, J., Strecker, G., Dorland, L., Haverkamp, J., Vliegenthardt, J.F.G., Binetter, J.P., and Schmid, K. (1978) Determination of the primary structures of 16 asialo-carbohydrate units derived from human plasma alpha 1-acid glycoprotein by 360 MHz 1H NMR spectroscopy and permethylation analysis. *Biochemistry*, **17**, 5206–5214.

Fournier, T., Medjoubi, N.N., and Porquert, D. (2000) Alpha-1-acid glycoprotein. *Biochim. Biophys. Acta*, **1482**, 157–171.

Fukui, S., Feizi, T., Galstian, C., Lawson, A.M., and Chai, W. (2002) Oligosaccharide microarrays for high-throughput detection and specificity assignments of carbohydrate-protein interactions. *Nature Biotechnol.*, **20**, 1011–1017.

Green, E.D., Adelt, G., Baenziger, J.U., Wilson, S., and Halbeek, H.V. (1988) The asparagine-linked oligosaccharides on bovine fetuin. Structural analysis of *N*-glycanase-released oligosaccharides by 500 MHz H1-NMR spectroscopy. *J. Biol. Chem.*, **263**, 18253–18268.

Hayase, T., Rice, K.G., Dziegielenwska, K.M., Kuhlenschmidt, M., Reilly, T., and Lee, Y.C. (1992) Comparison of *N*-glycosides of fetuins from different species and human alpha2-HS-glycoprotein. *Biochemistry*, **31**, 4915–4921.

Hochepied, T., Van Molle, W., Berger, F.G., Baumann, H., and Libert, C. (2000) Involvement of the acute phase protein alpha1-acid glycoprotein in nonspecific resistance to a lethal gram-negative infection. *J. Biol. Chem.*, **275**, 14903–14909.

Kakehi, K., Kinoshita, M., and Nakano, M. (2002) Analysis of glycoproteins and the oligosaccharides thereof by high-performance capillary electrophoresis—significance in regulatory studies on biopharmaceutical products. *Biomed. Chromatogr.*, **16**, 103–115.

Kawasaki, N., Itoh, S., Ohta, M., and Hayakawa, T. (2003) Microanalysis of *N*-linked oligosaccharides in a glycoprotein by capillary liquid chromatography/mass spectrometry and liquid chromatography/tandem mass spectrometry. *Anal. Biochem.*, **316**, 15–22.

Malykh, Y.N., King, T.P., Logan, E., Kelly, D., Schauer, R., and Shaw, L. (2003) Regulation of *N*-glycolylneuraminic acid biosynthesis in developing pig small intestine. *Biochem. J.*, **370**, 601–607.

Matsumoto, K., Nishi, K., Tokutomi, Y., Irie, T., Suenaga, A., and Otagiri, M. (2003) Effects of alpha 1-acid glycoprotein on erythrocyte deformability and membrane stabilization. *Biol. Pharm. Bull.*, **26**, 123–126.

Morimoto, N., Nakano, M., Kinoshita, M., Kawabata, A., Morita, M., Oda, Y., Kuroda, R., and Kakehi, K. (2001) Specific distribution of sialic acids in animal tissues as examined by LC-ESI-MS after derivatization with 1,2-diamino-4,5-methylenedioxybenzene. *Anal. Chem.*, **73**, 5422–5428.

Nakajima, K., Oda, Y., Kinoshita, M., and Kakehi, K. (2003) Capillary affinity electrophoresis for the screening of post-translational modification of proteins with carbohydrates. *J. Proteome Res.*, **2**, 81–88.

Nakano, M., Kakehi, K., and Lee, Y.C. (2003) Sample clean-up method for analysis of complex-type *N*-glycans released from glycopeptides. *J. Chromatogr. A*, **1005**, 13–21.

Sarcione, E.J. (1967) Hepatic synthesis and secretory release of plasma alpha-2 (acute phase)-globulin appearing in malignancy. *Cancer Res.*, **27**, 2025–2033.

Sato, C., Inoue, S., Matsuda, T., and Kitajima, K. (1998) Development of a highly sensitive chemical method for detecting α2-8-linked oligo/polysialic acid residues in glycoprotein blotted on the membrane. *Anal. Biochem.*, **261**, 191–197.

Sato, C., Inoue, S., Matsuda, T., and Kitajima, K. (1999) Fluorescent-assisted detection of oligosyalyl units in glycoconjugates. *Anal. Biochem.*, **266**, 102–109.

Schauer, R., Stoll, S., and Reuter, G. (1991) Differences in the amount of *N*-acetyl- and *N*-glycolyl-neuraminic acid, as well as *O*-acylated sialic acids, of fetal and adult bovine tissues. *Carbohydr. Res.*, **213**, 353–359.

Schmid, K., Nimberg, R.B., Kimura, A., Yamaguchi, H., and Binette, J.P. (1977) The carbohydrate units of human plasma alpha1-acid glycoprein. *Biochim. Biophys. Acta*, **492**, 291–302.

Sei, K., Nakano, M., Kinoshita, M., Masuko, T., and Kakehi, K. (2002) Collection of alpha1-acid glycoprotein molecular species by capillary electrophoresis and the analysis of their molecular mass and carbohydrate chains. *J. Chromatogr. A*, **985**, 273–281.

Sorensson, J., Matejka, G.L., Ohlson, M., and Haraldsson, B. (1999) Human endothelial cells produce orosomucoid, an important component of the capillary barrier. *Am. J. Physiol.*, **276**, H530–H534.

Stubbs, H.J., Shia, M.A., and Rice, K.G. (1997) Preparative purification of tetraantennary oligosaccharides from human asialyl orosomucoid. *Anal. Biochem.*, **247**, 357–365.

Townsend, R.R., Hardy, M.R., Wong, T.C., and Lee, Y.C. (1986) Binding of *N*-linked bovine fetuin glycopeptides to isolated rabbit hepatocytes: Gal/GalNAc hepatic lectin discrimination between Gal beta(1,4) GlcNAc and Gal beta(1,3)GlcNAc in a triantennary structure. *Biochemistry*, **25**, 5716–5725.

Treuheit, M.J., Costello, C.E., and Halsall, H.B. (1992) Analysis of the five glycosylation sites of human alpha 1-acid glycoprotein. *Biochem. J.*, **283**, 105–112.

GASTROENTEROLOGY 2004;126:208–219

A Protective Role of Protease-Activated Receptor 1 in Rat Gastric Mucosa

ATSUFUMI KAWABATA,* HIROYUKI NISHIKAWA,† HITOMI SAITOH,* YUMIKO NAKAYA,* KAORI HIRAMATSU,* SATOKO KUBO,* MINORU NISHIDA,† NAOYUKI KAWAO,* RYOTARO KURODA,* FUMIKO SEKIGUCHI,* MITSUHIRO KINOSHITA,§ KAZUAKI KAKEHI,§ NAOKI ARIZONO,‖ HISAKAZU YAMAGISHI,¶ and KENZO KAWAI†

Divisions of *Physiology and Pathophysiology and §Drug Information, School of Pharmaceutical Sciences, Kinki University, Higashi-Osaka; †Research and Development Center, Fuso Pharmaceutical Industries Ltd., Osaka; and Departments of ‖Zoology and ¶Digestive Surgery, Kyoto Prefectural University of Medicine, Kyoto, Japan

Background & Aims: On activation, protease-activated receptor (PAR)-2 modulates multiple gastric functions and exerts mucosal protection via activation of sensory neurons. The role of PAR-1, a thrombin receptor, in the stomach remains unknown. We thus examined if the PAR-1 agonist could protect against gastric mucosal injury in rats. *Methods:* Gastric mucosal injury was created by oral administration of ethanol/HCl or absolute ethanol in conscious rats. Gastric mucosal blood flow and acid secretion were determined in anesthetized rats. Immunohistochemical analyses of PAR-1 and cyclooxygenase (COX)-1 were also performed in rat and human stomach. *Results:* The PAR-1 agonist TFLLR-NH_2, administered intravenously in combination with amastatin, protected against the gastric mucosal injury induced by ethanol/HCl or absolute ethanol. The protective effect of TFLLR-NH_2 was abolished by indomethacin or a COX-1 inhibitor but not by ablation of sensory neurons with capsaicin. TFLLR-NH_2 produced an NO-independent increase in gastric mucosal blood flow that was partially inhibited by blockade of the endothelium-derived hyperpolarizing factor pathway. This inhibitory effect was promoted by indomethacin. TFLLR-NH_2 suppressed carbachol-evoked acid secretion in an indomethacin-reversible manner. Immunoreactive PAR-1 and COX-1 were expressed abundantly in rat gastric muscularis mucosae and smooth muscle, and the former protein was also detectable in blood vessels. Similar staining was observed in human gastric muscularis mucosae. *Conclusions:* The PAR-1 agonist, given systemically, protects against gastric mucosal injury via COX-1–dependent formation of prostanoids, modulating multiple gastric functions. Our data identify a novel protective role for PAR-1 in gastric mucosa, and the underlying mechanism is entirely different from that for PAR-2.

Protease-activated receptors (PARs) are G protein–coupled 7-transmembrane domain receptors that are activated by proteolytic unmasking of the cryptic tethered ligand present in the N-terminal domain. Among 4 PAR family members, PAR-1, PAR-2, and PAR-4 but not PAR-3 can be activated nonenzymatically by synthetic peptides as short as 5–6 amino acids based on the tethered ligand sequences.[1–5] PAR-1, PAR-3, and PAR-4 are thrombin receptors, whereas PAR-2 is a receptor activated by trypsin, mast cell tryptase, coagulation factors VIIa and Xa, and others.[6,7] PAR-1 and PAR-2 are expressed in a variety of tissues and cells, especially throughout the gastrointestinal tract.[6–8] PAR-2 is a plurifunctional receptor and now considered one of the key molecules in modulating alimentary functions.[6–8] PAR-2 is involved in salivary[9–11] and pancreatic[9,12,13] exocrine secretion, gastrointestinal smooth muscle motility modulation,[14–17] intestinal ion transport,[18] and modulation of gastric mucosal functions.[19] PAR-1 also modulates gastrointestinal smooth muscle motility[16,17,20,21] and ion transport in intestinal epithelial cells.[22] PAR-2, expressed in the capsaicin-sensitive sensory neurons,[23] not only triggers somatic pain and hyperalgesia[24,25] on activation but also appears to mediate visceral pain,[26] including pancreatic inflammatory pain.[27] Most recently, we found that the PAR-2–activating peptide SLIGRL-NH_2, administered systemically in combination with amastatin, an inhibitor of aminopeptidase, showed mucosal cytoprotective activity in rat gastric injury caused by ethanol/HCl or indomethacin, an effect mediated by activation of capsaicin-sensitive sensory neurons.[19] On activation, PAR-2 triggers neu-

Abbreviations used in this paper: COX, cyclooxygenase; GAPDH, glyceraldehyde-3-phosphate dehydrogenase; GMBF, gastric mucosal blood flow; L-NAME, N^G-nitro-L-arginine methyl ester; PAR, protease-activated receptor; RT-PCR, reverse-transcription polymerase chain reaction.

0016-5085/04/$30.00
doi:10.1053/j.gastro.2003.10.071

rally mediated mucus secretion,[19] enhances mucosal blood flow,[19] suppresses acid secretion,[28] and increases pepsinogen secretion.[29] In contrast, the roles of thrombin and PAR-1 in the gastric mucosa currently remain unknown. In this context, we investigated effects of the specific PAR-1–activating peptide TFLLR-NH_2 on gastric functions in vivo in rats. In humans and guinea pigs, the platelets of which express PAR-1, systemic administration of the PAR-1–activating peptide would induce serious intravascular platelet aggregation. In contrast, rat and mouse platelets do not express PAR-1 but PAR-3 and PAR-4 as thrombin receptors,[1,3–7] which enabled us to evaluate the effect of the peptide in rats in vivo. Although we do not expect clinical therapeutic application of PAR-1 agonists to gastric diseases, the present study would be useful to understand potential roles for PAR-1 in the gastric mucosa in mammals, including humans. In this context, we also performed immunohistochemical analysis of both rat and human gastric tissues. Here we show for the first time to our knowledge that the PAR-1–activating peptide exerts gastric mucosal protection and that the underlying mechanisms involve endogenous prostaglandins, differing from the neurally mediated protection caused by PAR-2 activation.

Materials and Methods

Experimental Animals

Male Wistar rats (7–8 weeks old; Japan SLC, Inc., Shizuoka, Japan) were housed in a temperature-controlled room, and food and water were provided ad libitum. All experimental protocols were approved by the Committee for the Care and Use of Laboratory Animals of the Kinki University School of Pharmaceutical Sciences.

Evaluation of Effect of the PAR-1–Activating Peptide in Rat Models for Gastric Injury

Two types of gastric mucosal lesion models were created by distinct injury inducers, ethanol/HCl and absolute ethanol, in unanesthetized rats after a 24-hour fast. The rat received 1.5 mL of 60% ethanol/150 mmol/L HCl solution or absolute ethanol orally and after 2 hours was killed by cervical exsanguination under ether anesthesia for observation of gastric injury. The stomach was excised, washed, and fixed with 10% formalin solution. The area of gastric glandular mucosal lesion was observed in digital photographs and measured with an image process program (Win Roof, Fukui, Japan) in a blinded evaluation. Lesion area is expressed as a percentage of the total area of the stomach except for the fundus. Peptides were administered intravenously (IV) 5 minutes before challenge with the injury inducer. Amastatin, an inhibitor of aminopeptidase that degrades peptides, was administered IV 1 minute before peptide administration.

Measurements of Gastric Mucosal Blood Flow and Mean Arterial Blood Pressure in Anesthetized Rats

In the rat anesthetized with 1.5 g/kg urethane intraperitoneally, gastric mucosal blood flow (GMBF) was determined after a 24-hour fast using a laser Doppler flowmeter (ALF-21; Advance Co., Tokyo, Japan). A probe (type N; Advance Co.) was placed lightly on the surface of the corpus mucosa through a balancer (ALF-B; Advance Co.) as reported previously.[19] The left carotid artery was cannulated with a polyethylene tube containing isotonic heparin solution (5 U/mL) that was connected with a pressure transducer (DTX Plus DT-XXAD; Becton Dickinson Critical Care System Pty Ltd., Singapore) for continuous monitoring of mean arterial blood pressure. Peptides were administered IV after a stabilization period.

Determination of Gastric Acid Secretion in Anesthetized Rats

After a 24-hour fast, the rat was anesthetized with 1.5 g/kg urethane intraperitoneally and tracheotomized, and the gastric lumen was perfused through 2 polyethylene cannulae. As described by Takeuchi et al.,[30] a cannula was inserted into the forestomach through the esophagus and cardia and the other into the pyloric region through the duodenum. The stomach was perfused at a flow rate of 1 mL/min with saline solution that was adjusted to pH 7.0 and gassed with 100% oxygen. The luminal acid content was determined by titration to pH 7.0 with 0.05N sodium hydroxide using a pH statmeter (pH Stat AUT-211; DKK-TOA Corp., Tokyo, Japan). After a stabilization period, 60 μg/kg carbachol was administered subcutaneously (SC); the PAR-1 agonist TFLLR-NH_2 or the control peptide FTLLR-NH_2 (100–1000 nmol/kg) in combination with 2.5 μmol/kg amastatin was administered IV 30 minutes after the injection of carbachol, at which the carbachol-evoked acid output peaked.

Inhibition Experiments In Vivo

The nitric oxide synthase inhibitor N^G-nitro-L-arginine methyl ester (L-NAME) (30 mg/kg)[19] and the cyclooxygenase (COX) inhibitor indomethacin (20 mg/kg)[31] were administered intraperitoneally 5 minutes and SC 30 minutes, respectively, before IV administration of peptides. The COX-1 selective inhibitor SC-560 (10 mg/kg) or the COX-2 selective inhibitor NS-398 (5 mg/kg) was administered SC 30 minutes before IV administration of peptides. Apamin (an inhibitor of small-conductance, Ca^{2+}-activated K^+ channels) in combination with charybdotoxin (an inhibitor of large- and intermediate-conductance, Ca^{2+}-activated K^+ channels), each at 0.05 mg/kg,[8,32] was administered IV 20 minutes before the peptide challenge. For ablation of sensory nerves, capsaicin at 25, 50, and 50 mg/kg was administered SC to the rat under pentobarbital (40 mg/kg intraperitoneally) anesthesia 3 times at 0,

6, and 32 hours, respectively (125 mg/kg in all); the rat was used for experiments 10 days after the final dose. The effectiveness of the capsaicin treatment was confirmed as described previously.[23]

Measurements of the Relaxant Activity of the PAR-1 Agonist in Isolated Rat Gastric Longitudinal Smooth Muscle

The rat was killed by decapitation, and the stomach was excised. The mucosa-removed gastric strip (5 × 15 mm) was prepared and equilibrated for 1 hour at 37°C under a load of 10 mN in a gassed (95% O_2/5% CO_2) Krebs-Henseleit solution of the following composition (in mmol/L): 118 NaCl, 4.7 KCl, 2.5 $CaCl_2$, 1.2 $MgCl_2$, 25 $NaHCO_3$, 1.2 KH_2PO_4, and 10 glucose. The isometric tension of the longitudinal smooth muscle preparation was monitored as described elsewhere.[14,21] In inhibition experiments, 10 μmol/L indomethacin, 0.1 μmol/L apamin, or 0.1 μmol/L charybdotoxin was applied to the tissue 5 minutes before the addition of carbachol.

Immunostaining of PAR-1 and COX-1 in Rat Stomach

Under ether anesthesia, the rat was perfused transcardially with physiologic saline and the stomach quickly removed for immunohistochemical analyses of PAR-1 and COX-1. The isolated tissue was embedded in OTC compound (Tissue-Tek; Miles Inc., Torrance, CA), snap frozen, and serially sectioned (5-μm thickness) using Cryocut (Leica Microsystems Nussloch GmbH, Baden-Württemberg, Germany). Polyclonal anti–PAR-1 and anti–COX-1 antibodies (Santa Cruz Biotechnology, Inc., Santa Cruz, CA) were used as the primary antibody. The sections were incubated in 10% normal rabbit serum (Nichirei Corp., Tokyo, Japan) and then in the primary antibody to PAR-1 or COX-1 at 4 μg/mL for 2 hours at room temperature. The bound primary antibodies were detected using Histofine Simple Stain MAX-PO (Nichirei Corp.). The labeled cells were visualized by 3,3′-diaminobenzidine tetrahydrochloride (DakoCytomation Co. Ltd., Kyoto, Japan) and 0.03% hydrogen peroxide. The sections were lightly counterstained with hematoxylin. In blocking experiments, the diluted primary antibody was preincubated for 24 hours at 4°C with 20 μg/mL of each blocking peptide (Santa Cruz Biotechnology, Inc.).

Reverse-Transcription Polymerase Chain Reaction Analysis of PAR-1 Messenger RNA and Immunostaining of PAR-1 and COX-1 in Human Stomach

Normal tissue parts were visually identified and collected from the whole stomach that was surgically isolated from a patient with gastric cancer (a 51-year-old man) after obtaining informed consent. The tissue was separated into the gastric mucosa with the muscularis mucosae and the smooth muscle layer. The tissue specimens were used for immunohistochemical analyses of PAR-1 and COX-1 and also for reverse-transcription polymerase chain reaction (RT-PCR) analysis. Immunostaining of PAR-1 and COX-1 was performed using the same primary antibodies as previously mentioned according to almost the same protocol as that for rat tissues; the concentrations of the primary antibodies to PAR-1 and COX-1 were 4 and 0.4 μg/mL, respectively.

The tissue specimens for RT-PCR analysis were stored in an RNA stabilization solution (RNAlater; Ambion, Austin, TX) at 4°C for a few days. Total RNA was reverse transcribed at 42°C for 50 minutes and amplified by PCR using the RNA LA PCR kit (AMV) version 1.1 (Takara, Japan). Amplification was performed using a 30-second denaturation period at 94°C, a 30-second reannealing period at 55°C, and a 1-minute primer extension period at 72°C. The PCR amplification for PAR-1 and glyceraldehyde-3-phosphate dehydrogenase (GAPDH) was allowed to proceed for 40–45 cycles and 35 cycles, respectively. The primer pairs used were 5′-TGTGAACT-GATCATGTTTATG-3′ (forward) and 5′-TTCGTAA-GATAAGAGATATGT-3′ (reverse) for PAR-1 and 5′-GAC-CCCTTCATTGACCTCAACTACATG-3′ (forward) and 5′-GTCCACCACCCTGTTGCTGTAGCC-3′ (reverse) for GAPDH, yielding amplification of 708– and 876–base pair fragments, respectively. The PCR products were separated using 2% agarose gel electrophoresis and visualized by ethidium bromide staining.

Chemicals

PAR-related peptides were prepared by a standard solid-phase synthesis procedure. The concentration, purity, and composition of the peptides were determined by high-performance liquid chromatography, mass spectrometry, and quantitative amino acid analysis. Capsaicin, L-NAME hydrochloride, carbachol, and apamin were purchased from Sigma Chemical Co. (St. Louis, MO), and indomethacin and charybdotoxin were obtained from Wako Pure Chem. (Osaka, Japan) and Peptide Institute, Inc. (Minoh, Japan), respectively. SC-560 and NS-398 were obtained from Cayman Chemical (Ann Arbor, MI). Capsaicin was dissolved in a saline solution containing 10% ethanol and 10% Tween 80, and SC-560 and NS-398 were dissolved in dimethyl sulfoxide. Indomethacin was dissolved in 4% sodium bicarbonate. All other chemicals, including peptides, were dissolved in saline. Control animals received administration of each vehicle.

Statistical Analysis

Data are represented as means with SEM. Statistical significance was analyzed by the Student t test for comparison between 2 groups and by analysis of variance followed by Tukey's test for multiple comparisons and was set at a level of $P < 0.05$.

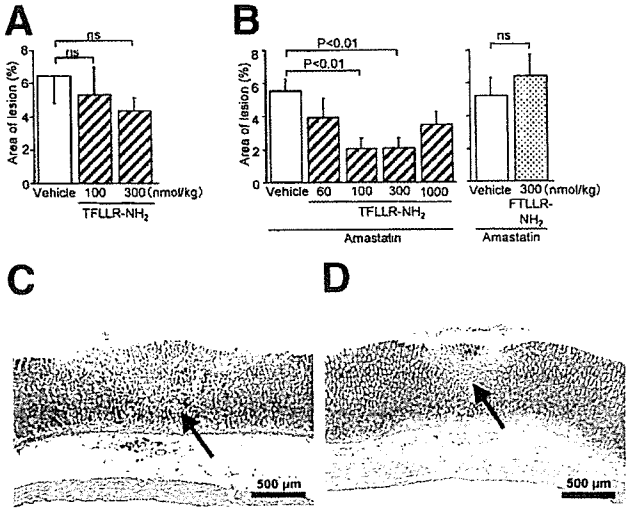

Figure 1. Protective effects of the PAR-1–activating peptide TFLLR-NH_2 on the gastric mucosal lesions induced by 60% ethanol/150 mmol/L HCl in conscious rats. TFLLR-NH_2 or FTLLR-NH_2, an inactive control peptide, (*A*) without or (*B*) with IV preadministration of 2.5 μmol/kg amastatin was administered IV 5 minutes before oral administration of ethanol/HCl. (*C* and *D*) Typical photomicrographs of the center of the injured area induced by ethanol/HCl in the rats treated with amastatin plus vehicle and amastatin plus TFLLR-NH_2 at 300 nmol/kg, respectively. *Arrows* show the injured area. Data show the mean with SEM from (*A*) 6 or (*B*) 9–15 rats. ns, not significant.

Results

Protective Effect of Systemic Administration of the PAR-1–Activating Peptide Against the Gastric Injury Caused by Ethanol/HCl in Conscious Rats

The PAR-1–activating peptide TFLLR-NH_2, when administered IV at 100 and 300 nmol/kg, tended to reduce the gastric lesion induced by ethanol/HCl in conscious rats, but no significant effect was detected (Figure 1*A*). We then examined the effect of the peptide in combination with amastatin, an inhibitor of aminopeptidase known to quickly degrade and inactivate peptides. IV TFLLR-NH_2 (60–300 nmol/kg) in combination with 2.5 μmol/kg IV amastatin strongly suppressed the gastric lesions in a dose-dependent manner (Figure 1*B*), whereas amastatin itself had no effect (Figure 1*A* and *B*). The highest dose of TFLLR-NH_2 exhibited a relatively reduced protective effect (Figure 1*B*). The typical photomicrographs in the center of the injured area in the stomach also show that the extent of the gastric mucosal lesion in the rat treated with 300 nmol/kg TFLLR-NH_2 plus amastatin (Figure 1*D*) was less serious than that in the control rat (Figure 1*C*). Of note is that the partially reversed inactive peptide FTLLR-NH_2 (300 nmol/kg), coadministered with amastatin, had no effect in this gastric injury model (Figure 1*B*, right).

To determine the mechanisms underlying the mucosal protection exerted by the PAR-1–activating peptide in combination with amastatin in the ethanol/HCl-induced gastric injury model, inhibition experiments were performed. Because capsaicin-sensitive sensory neurons are known to contribute to the gastric mucosal cytoprotection exerted by the PAR-2–activating peptide SLIGRL-NH_2,[19] we tested the effect of TFLLR-NH_2 in the rat that had received large doses of capsaicin for ablation of sensory neurons. Although treatment with capsaicin itself augmented the ethanol/HCl-evoked gastric lesions, the protective actions of 300 nmol/kg TFLLR-NH_2 were not blocked by treatment with capsaicin (Figure 2*A*), indicating involvement of mechanisms distinct from those for PAR-2 agonists.[19] The NO synthase inhibitor L-NAME (30 mg/kg) also failed to abolish the mucosal protection caused by TFLLR-NH_2, although L-NAME itself facilitated the ethanol/HCl-evoked gastric lesions (Figure 2*B*). In contrast, indomethacin (20 mg/kg), a nonselective COX inhibitor, enhanced the ethanol/HCl-evoked gastric lesions and abolished the protective effect of TFLLR-NH_2 (Figure 2*C*). Similarly, the COX-1–selective inhibitor SC-560 (5 mg/kg), but not the COX-2–selective inhibitor NS-398 (10 mg/kg), blocked the gastric mucosal protection exerted by TFLLR-NH_2 (Figure 3).

Mucosal Protection by PAR-1 Activation in the Gastric Injury Induced by Absolute Ethanol in Conscious Rats

We next determined if the PAR-1–activating peptide TFLLR-NH_2 could exhibit gastric protective activity in the gastric lesions induced by absolute ethanol, without administration of exogenous HCl, in con-

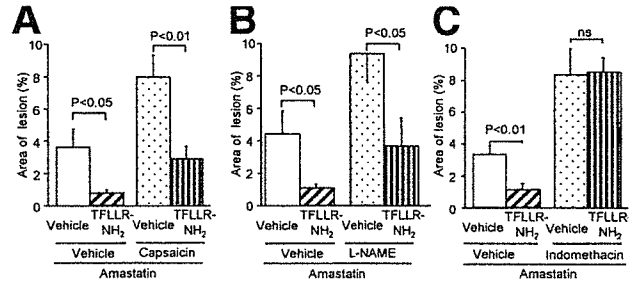

Figure 2. Effects of capsaicin, L-NAME, or indomethacin on the protection by the PAR-1 agonist TFLLR-NH_2 against the gastric mucosal injury induced by 60% ethanol/150 mmol/L HCl in conscious rats. (*A*) Capsaicin at a total dose of 125 mg/kg was administered SC 10 days before experiments were performed. (*B*) L-NAME (30 mg/kg) and (*C*) indomethacin (20 mg/kg) were administered intraperitoneally 5 minutes and SC 30 minutes, respectively, before IV TFLLR-NH_2 (300 nmol/kg). Data show the mean with SEM from (*A*) 5–6, (*B*) 9–10, or (*C*) 17 rats. ns, not significant.

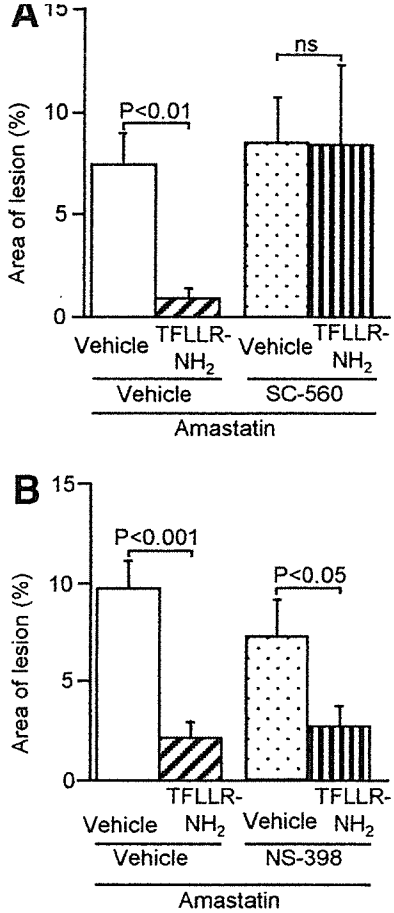

Figure 3. Effects of the COX-1 inhibitor SC-560 and the COX-2 inhibitor NS-398 on the protection by the PAR-1 agonist TFLLR-NH_2 against the gastric mucosal injury induced by 60% ethanol/150 mmol/L HCl in conscious rats. (*A*) SC-560 (5 mg/kg) or (*B*) NS-398 (10 mg/kg) was administered SC 30 minutes before IV TFLLR-NH_2 (300 nmol/kg). Data show the mean with SEM from (*A*) 4 or (*B*) 11 rats. ns, not significant.

scious rats. TFLLR-NH_2 but not FTLLR-NH_2, a control peptide, when administered IV at 300 nmol/kg in combination with amastatin, strongly attenuated the gastric lesions induced by absolute ethanol (Figure 4*A*). The protective effect of TFLLR-NH_2 was completely inhibited by pretreatment with 20 mg/kg indomethacin (Figure 4*B*).

Enhancement of Gastric Mucosal Blood Flow Caused by the PAR-1–Activating Peptide in Anesthetized Rats

The PAR-1–activating peptide TFLLR-NH_2, administered IV with or without amastatin, produced transient increases in GMBF in anesthetized rats (Figure 5*A* and *B*). The effective dose ranges of TFLLR-NH_2 were 100 nmol/kg or more in the absence of amastatin (Figure 5*B*) and 30 nmol/kg or more in the presence of amastatin (Figure 5*A*). Clear dose-response relationships were not detected in these experiments (Figure 5*A* and *B*). The PAR-2–activating peptide SLIGRL-NH_2 (300 nmol/kg), without amastatin, produced an increase in GMBF equivalent to that caused by TFLLR-NH_2 at 100–1000 nmol/kg (Figure 5*B* and *C*). SLIGRL-NH_2 (300 nmol/kg) also produced a considerable decrease in mean arterial blood pressure (Figure 5*C*), whereas TFLLR-NH_2 (300–1000 nmol/kg) caused only a transient slight decrease in mean arterial blood pressure (Figure 5*B*). Thus, it is noteworthy that the effect of the PAR-1 agonist might be relatively specific for gastric microcirculation.

To determine the mechanisms underlying the enhancement of GMBF by the PAR-1–activating peptide, inhibition experiments were performed in anesthetized rats. The increase in GMBF caused by TFLLR-NH_2 (300 nmol/kg) was resistant to pretreatment with the NO synthase inhibitor L-NAME (Figure 6*A*). Indomethacin showed only a slight tendency toward reducing the enhancement of GMBF caused by TFLLR-NH_2 (Figure

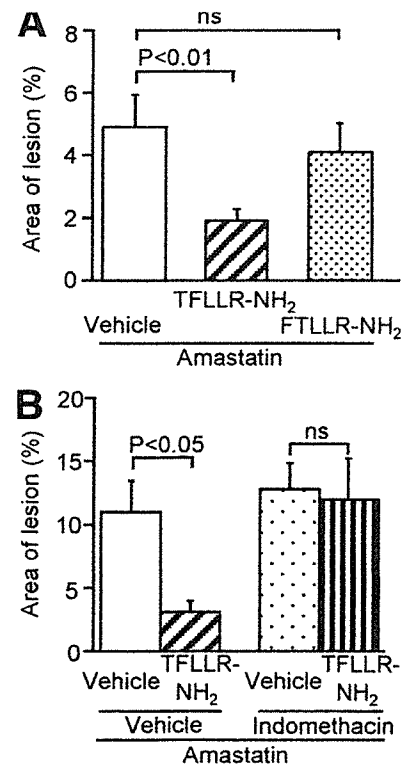

Figure 4. Protective effects of the PAR-1–activating peptide TFLLR-NH_2 on the gastric mucosal lesions induced by absolute ethanol in conscious rats. (*A*) TFLLR-NH_2 or FTLLR-NH_2, an inactive control peptide, at 300 nmol/kg in combination with 2.5 μmol/kg amastatin was administered IV 5 minutes before oral administration of absolute ethanol. (*B*) Indomethacin (20 mg/kg) was administered SC 30 minutes before IV TFLLR-NH_2 (300 nmol/kg). Data show the mean with SEM from (*A*) 18 (vehicle) or 12–13 (peptide) rats and from (*B*) 8–14 rats. ns, not significant.

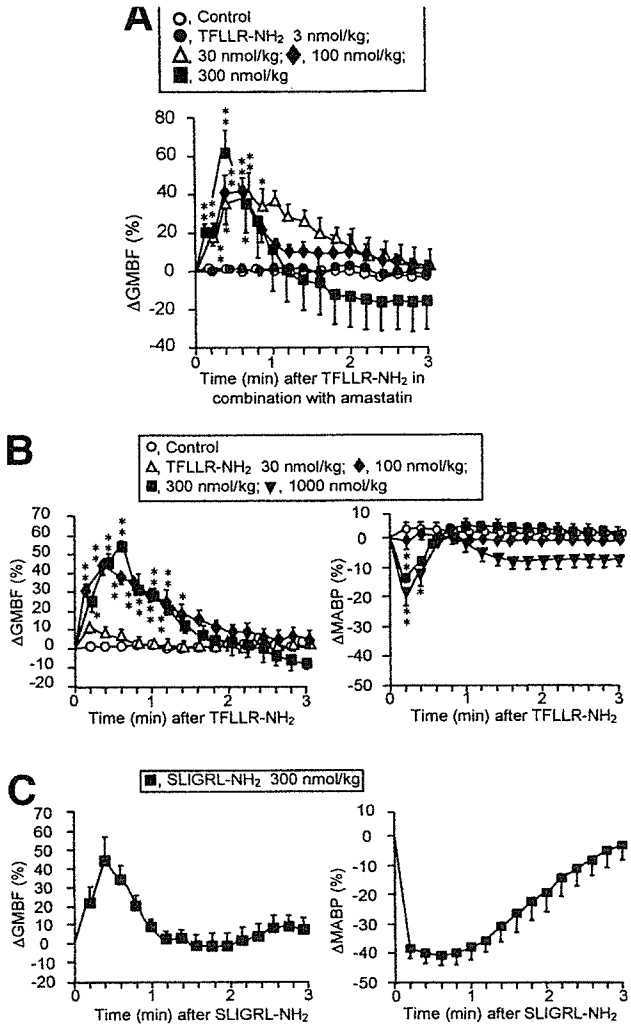

Figure 5. Effects of the PAR-1 agonist TFLLR-NH_2 on GMBF in anesthetized rats. TFLLR-NH_2 or the PAR-2 agonist SLIGRL-NH_2, (*A*) with or (*B* and *C*) without preadministration of 2.5 μmol/kg amastatin, was administered IV to the rat, and changes in GMBF and/or mean arterial blood pressure were monitored. Data show the mean with SEM from 4–9 rats. $*P < 0.05$, $**P < 0.01$ vs. control.

6*B*). We next tested the effect of combined administration of apamin and charybdotoxin, inhibitors of distinct types of Ca^{2+}-activated K^+ channels known to abolish vascular relaxation via endothelium-derived hyperpolarizing factor in vitro and in vivo,[32,33] because the PAR-2–mediated increase in GMBF was abolished by these 2 K^+ channel inhibitors.[8] Apamin (0.05 mg/kg) in combination with charybdotoxin (0.05 mg/kg) partially inhibited the TFLLR-NH_2–evoked increase in GMBF, whereas the early phase of the increase in GMBF (0–36 seconds after administration of TFLLR-NH_2) was resistant to apamin plus charybdotoxin (Figure 6*C*). Combined administration of indomethacin in addition to apamin plus charybdotoxin produced greater inhibition of the TFLLR-NH_2–evoked increase in GMBF, although complete inhibition was still not obtained (Figure 6*D*).

Inhibition by the PAR-1–Activating Peptide of Carbachol-Evoked Gastric Acid Secretion in Anesthetized Rats

In the anesthetized rat, IV injection of 1000 nmol/kg TFLLR-NH_2 in combination with amastatin tended to reduce the basic acid secretion, while statistical significance was not obtained every 10 minutes and also over 120 minutes after IV administration; the total value of acid output over 120 minutes (μmol/120 min) was 13.0 ± 4.7 and 2.05 ± 1.46 in the groups treated with vehicle and 1000 nmol/kg TFLLR-NH_2, respectively ($n = 5$; $P = 0.077$).

SC injection of 60 μg/kg carbachol evoked a prompt secretion of acid, an effect peaking at 30 minutes and lasting for more than 120 minutes (Figure 7*A*). TFLLR-NH_2 at 300 and 1000 nmol/kg but not 100 nmol/kg administered in combination with amastatin at a peak time, 30 minutes after SC carbachol, significantly suppressed the evoked acid output. The control peptide FTLLR-NH_2 (1000 nmol/kg) in combination with amastatin had no such effect (Figure 7*A*). The inhibition

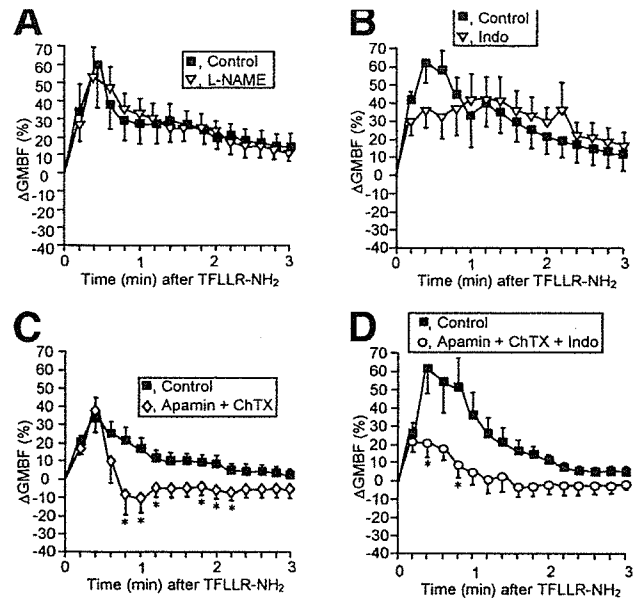

Figure 6. Effects of some inhibitors on the increase in GMBF caused by the PAR-1 agonist TFLLR-NH_2 in anesthetized rats. Inhibitory effects of (*A*) L-NAME, (*B*) indomethacin (Indo), (*C*) apamin plus charybdotoxin (ChTX), or (*D*) apamin plus charybdotoxin plus indomethacin on the PAR-1–mediated increase in GMBF were examined. Rats received 30 mg/kg IV L-NAME, 20 mg/kg SC indomethacin, and 0.05 mg/kg IV apamin plus 0.05 mg/kg charybdotoxin 5, 30, and 20 minutes, respectively, before 300 nmol/kg IV TFLLR-NH_2. Data show the mean with SEM from 8–13 rats. $*P < 0.05$ vs. control.

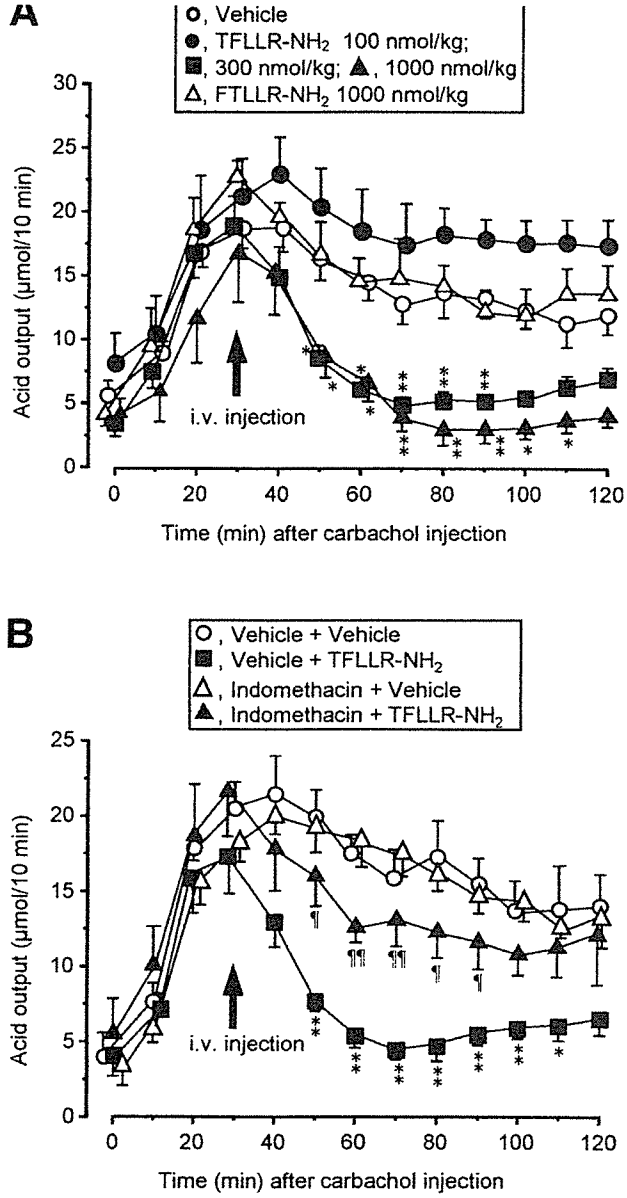

Figure 7. Inhibitory effects of the PAR-1 agonist TFLLR-NH_2 on carbachol-evoked acid secretion in anesthetized rats. (*A*) TFLLR-NH_2 or FTLLR-NH_2 in combination with 2.5 μmol/kg amastatin was administered IV 30 minutes after 60 μg/kg SC carbachol. (*B*) Indomethacin (20 mg/kg) was administered SC immediately before carbachol (30 minutes before IV TFLLR-NH_2 at 1000 nmol/kg in combination with amastatin). Data show the mean with SEM from (*A*) 9 (vehicle) or 4–5 (peptides) rats and from (*B*) 5–6 rats. $*P < 0.05$, $**P < 0.01$ vs. (*A*) vehicle or (*B*) vehicle plus vehicle; $¶P < 0.05$, $¶¶P < 0.01$ vs. vehicle plus TFLLR-NH_2.

by 1000 nmol/kg TFLLR-NH_2 of carbachol-evoked acid secretion was largely blocked by preadministration of 20 mg/kg indomethacin, although indomethacin itself did not affect the carbachol-evoked acid secretion (Figure 7*B*).

Effects of the PAR-1–Activating Peptide on Tension of the Isolated Rat Gastric Longitudinal Strip In Vitro

The PAR-1 agonist TFLLR-NH_2 (1–100 μmol/L) contracted the rat gastric longitudinal smooth muscle preparation in a concentration-dependent manner, as described previously,[20] whereas the PAR-2 agonist SLIGRL-NH_2 in the same concentration range produced no contraction in the same preparation in our experimental conditions (data not shown). The contractile response to TFLLR-NH_2 (1–100 μmol/L) was not significantly altered by 10 μmol/L indomethacin; the contractile responses (% KCl) to 100 μmol/L TFLLR-NH_2 were 54.0 ± 15.7 (n = 4) and 57.3 ± 11.1 (n = 4) in the absence and presence of indomethacin, respectively.

In the rat gastric longitudinal strip precontracted with 0.3 μmol/L carbachol, 0.1–10 μmol/L TFLLR-NH_2 and 1–100 μmol/L SLIGRL-NH_2 produced relaxation responses in a concentration-dependent manner, as shown in the mouse gastric longitudinal strip.[16] The relaxant effects of 10 μmol/L TFLLR-NH_2 and 100 μmol/L SLIGRL-NH_2 were abolished by 0.1 μmol/L apamin but not by 10 μmol/L indomethacin, in agreement with the previous evidence in the mouse preparation[16]; in the absence (control) and presence of apamin and indomethacin, the relaxation responses (% carbachol) to TFLLR-NH_2 were 39.2 ± 3.5 (n = 12), 2.3 ± 2.3 ($P < 0.01$ vs. control; n = 4), and 39.8 ± 4.4 (n = 4), respectively, and those to SLIGRL-NH_2 were 43.1 ± 3.9 (n = 12), 11.2 ± 5.2 ($P < 0.01$ vs. control; n = 4), and 40.4 ± 6.1 (n = 4), respectively.

Immunohistochemical Localization of PAR-1 and COX-1 in Rat Stomach

Immunohistochemical analysis of the rat stomach with the anti–PAR-1 polyclonal antibody showed that immunoreactive PAR-1 was abundantly expressed in the smooth muscle layer and muscularis mucosae (Figure 8*A*). In the gastric mucosal layer, the muscularis mucosae and blood vessels were stained clearly with the antibody (Figure 8*B*). All of this staining completely disappeared by preincubation of the antibody with a blocking peptide (Figure 8*C* and *D*). Immunostaining of COX-1 in the rat stomach showed that immunoreactive COX-1 was also present in the muscularis mucosae (Figure 9*A* and *B*), and the staining was abolished by a blocking peptide (Figure 9*C* and *D*). The immunostaining of COX-1 in gastric cells or regions other than the muscularis mucosa was not clear (Figure 9).

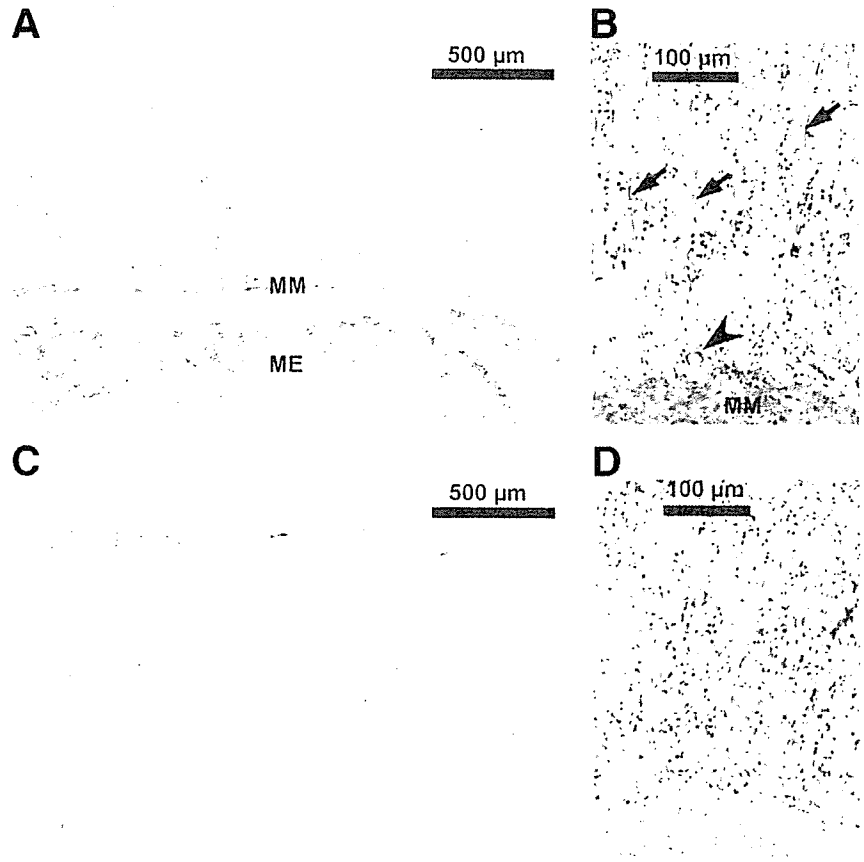

Figure 8. Immunohistochemical localization of PAR-1 in rat stomach. (*A* and *B*) Sections were incubated with the anti–PAR-1 polyclonal antibody. (*C* and *D*) Sections were stained with the antibody preincubated with a blocking peptide at 20 μg/mL. MM, muscularis mucosae; ME, muscularis externa. *Arrows* show muscularis mucosae within the mucosal layer, and an *arrowhead* indicates the blood vessel.

RT-PCR Detection of PAR-1 Messenger RNA and Immunohistochemical Localization of PAR-1 and COX-1 in Human Stomach

The signals of PCR products for human PAR-1 messenger RNA after 45-cycle amplification were detected in both the smooth muscle and the mucosa with the muscularis mucosae, although those after 40-cycle amplification were detectable in the former specimen but not the latter (Figure 10*A*). Immunohistochemical analysis of human gastric mucosa with the muscularis mucosae showed that immunoreactive PAR-1 was abundant in the muscularis mucosae and also present in the blood vessels (Figure 10*B* and *C*), as indicated in comparison with the experiments using the blocking peptide (Figure 10*D* and *E*). The positive signal on the mucosal surface (Figure 10*B*) is not considered specific staining, because it was not blocked by the absorption experiments (Figure 10*D*). COX-1 immunoreactivity was also positive in the muscularis mucosae (Figure 10*F* and *G*), which was abolished by the blocking peptide (Figure 10*H* and *I*). Thus, the distribution of immunoreactive PAR-1 and COX-1 in human stomach (Figure 10*B–I*) corresponded to that in rat stomach as shown in Figures 8 and 9.

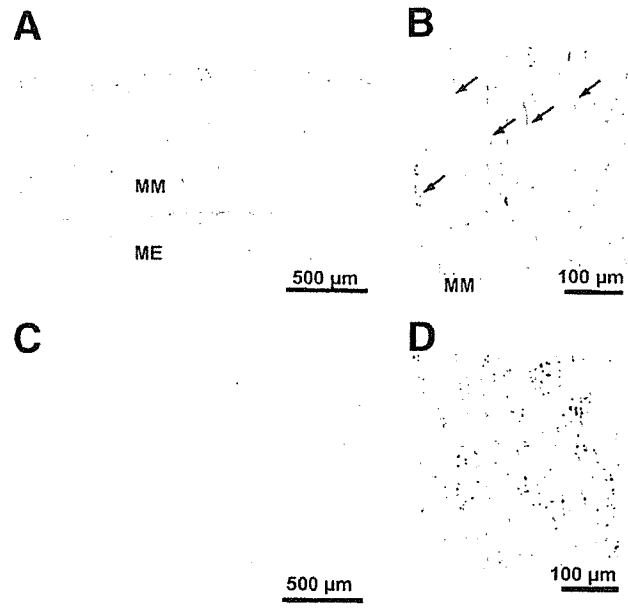

Figure 9. Immunohistochemical localization of COX-1 in rat stomach. (*A* and *B*) Sections were incubated with the anti–COX-1 polyclonal antibody. (*C* and *D*) Sections were stained with the antibody preincubated with a blocking peptide at 20 μg/mL. MM, muscularis mucosae; ME, muscularis externa. *Arrows* show muscularis mucosae within the mucosal layer.

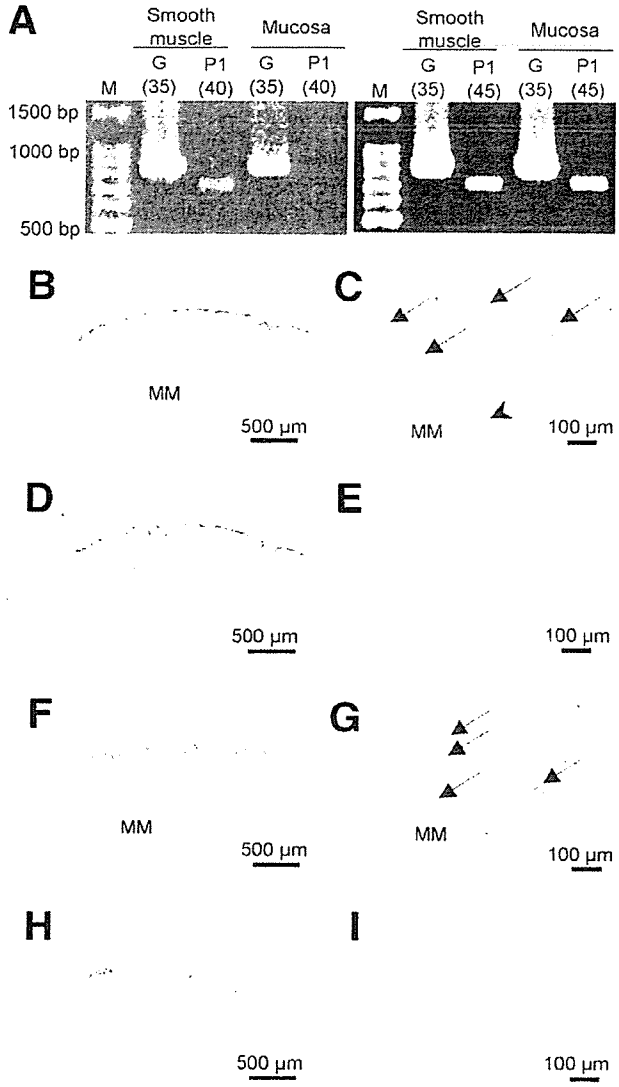

Figure 10. (*A*) RT-PCR analysis of PAR-1 messenger RNA in the smooth muscle and the mucosa with the muscularis mucosae of human stomach. M, marker; G, GAPDH; P1, PAR-1. *Parentheses* show the number of PCR cycles. (*B* and *C*) Immunohistochemical localization of PAR-1 in the muscularis mucosae of human stomach. (*D* and *E*) Blocking experiments. The PAR-1 antibody was preincubated with a blocking peptide at 20 μg/mL. (*F* and *G*) Immunohistochemical localization of COX-1 in the muscularis mucosae of human stomach. (*H* and *I*) Blocking experiments. The COX-1 antibody was preincubated with a blocking peptide at 2 μg/mL. MM, muscularis mucosae. *Arrows* show muscularis mucosae within the mucosal layer, and an *arrowhead* shows the blood vessel.

Discussion

The present study shows for the first time to our knowledge that the PAR-1 agonist administered systemically exerts gastric mucosal protection in rat gastric injury models. Our data also suggest that endogenous prostanoids produced by COX-1 but not sensory neurons are involved in PAR-1–mediated gastric mucosal protection, a mechanism differing from PAR-2–mediated gastric mucosal protection via activation of capsaicin-sensitive sensory neurons in the rat.[19] Our data also provide novel evidence for PAR-1 modulation of multiple functions, including GMBF and gastric acid secretion. Taken together, PAR-1, expressed in rat gastric tissues, modulates multiple gastric functions, playing a protective role in gastric mucosa through enhancement of prostanoid formation.

The specificity of TFLLR-NH_2 for PAR-1 is 220-fold higher than that for PAR-2 in vitro, and our in vivo study has shown that TFLLR-NH_2 (5 μmol/kg or less) has no agonistic activity for PAR-2.[9] The protective effect of TFLLR-NH_2 required concurrent administration of amastatin, an inhibitor of aminopeptidase that nonspecifically degrades peptides, in agreement with our study using SLIGRL-NH_2.[19] Therefore, continuous activation of PAR-1 might be necessary to achieve mucosal protection, because amastatin causes not only facilitation but also prolongation of effects of peptides in vivo.[9,34] Nonpeptide agonists or aminopeptidase-resistant peptide agonists for PAR-1, if any, would exert gastric mucosal cytoprotection without combined administration of amastatin.

The PAR-2 agonist exerts mucosal protection by activating capsaicin-sensitive sensory neurons in rat gastric injury models induced by ethanol/HCl or indomethacin.[19] PAR-1 and PAR-2 are expressed in the capsaicin-sensitive sensory neurons,[23,35] and activation of either receptor seems to trigger release of neuropeptides,[19,23,35] leading to our original expectation that PAR-1–mediated gastric mucosal protection might also involve neuronal mechanisms. An explanation is that sensory neurons present in the stomach might express PAR-2 but not PAR-1, although our present and previous[29] immunohistochemical analyses of gastric PAR-1 and PAR-2 failed to clarify distinct neuronal expression of these receptors in the stomach. Another possibility is that neuronal PAR-1 and PAR-2 might play distinct roles in gastric mucosa. Actually, it has been reported independently by us[24,36] and by Vergnolle et al.[25,35] that PAR-2 and PAR-1 in capsaicin-sensitive sensory neurons play distinct roles in processing of pain information (pronociceptive and antinociceptive, respectively).

The indomethacin-sensitive, antiacid secretion effect of TFLLR-NH_2 might explain the mechanisms underlying its protective effect against the absolute ethanol-induced gastric mucosal damage. However, this notion does not interpret the protective effect of TFLLR-NH_2 against the mucosal injury produced by exogenously applied acid (HCl) in addition to ethanol. Of interest is

Table 1. Summary of the Actions of Activation of PAR-1 or PAR-2 and the Underlying Mechanisms

	Action (mechanism)	
Function	PAR-1	PAR-2
Mucosal integrity	Protective (via prostanoid formation)	Protective (via activation of capsaicin-sensitive sensory neurons)
Acid secretion	Suppressive (via prostanoid formation)	Suppressive (via unknown mechanisms)
GMBF	Increase (via endothelium-derived hyperpolarizing factor, prostaglandins, and unknown mechanisms)	Increase (dependent on endothelium-derived hyperpolarizing factor)
Gastric smooth muscle	Contraction and relaxation (via activation of apamin-sensitive K^+ channels)	Relaxation (via activation of apamin-sensitive K^+ channels)

that the PAR-2 agonist SLIGRL-NH_2 suppresses the acid secretion induced by carbachol, pentagastrin, or 2-deoxy-D-glucose in an indomethacin-resistant manner,[28] although the underlying mechanisms have yet to be elucidated. Thus, on activation, PAR-1 and PAR-2 suppress acid secretion by prostanoid-dependent and -independent mechanisms, respectively.

It is also likely that the increased GMBF caused by TFLLR-NH_2 might contribute to its protective effect in gastric mucosa. The magnitude of the increase in GMBF caused by the PAR-1 and PAR-2 agonists was almost equivalent, whereas the PAR-1 agonist-triggered hypotension was much less than that caused by the PAR-2 agonist, implying that the PAR-1 agonist might act relatively specifically on gastric blood vessels. PAR-1 is expressed in vascular endothelium and, on activation, causes NO-dependent relaxation in isolated large blood vessels.[37] Nevertheless, our data suggest that the PAR-1–mediated increase in GMBF is independent of NO but partially mediated by prostanoids and endothelium-derived hyperpolarizing factor, known to be more important in endothelium-dependent relaxation in resistant blood vessels.[38] The mechanisms for the component of the increase in GMBF resistant to apamin/charybdotoxin/indomethacin are still open to question. The fact that indomethacin itself completely inhibited the mucosal protection but not the increase in GMBF exerted by the PAR-1 agonist suggests that the PAR-1–mediated increase in GMBF might play only a minor role in mucosal protection.

The finding that the PAR-1 agonist caused both contraction and apamin-sensitive relaxation in isolated rat gastric longitudinal smooth muscle in an indomethacin-resistant manner is in agreement with the previous studies using guinea pig and mouse longitudinal muscle.[16,39] Thus, the modulation by PAR-1 of gastric smooth muscle motility, such as facilitation of gastric emptying, is not considered to be involved in PAR-1–mediated, prostanoid-dependent protection against gastric mucosal injury.

The immunohistochemical finding that gastric muscularis mucosae and smooth muscle layers in the rat were abundant in immunoreactive PAR-1 is consistent with the fact that activation of PAR-1 produced both contraction and relaxation in rat gastric longitudinal smooth muscle as previously described. In the mucosal layer, however, PAR-1 immunoreactivity was detected in the muscularis mucosae projecting into the mucosa and in blood vessels. Because the gastric muscularis mucosae was also abundant in immunoreactive COX-1, it is likely that PAR-1–triggered gastric mucosal protection is mediated by production of prostanoids by COX-1 following activation of PAR-1 in gastric muscularis mucosae. The fact that the immunostaining of PAR-1 and COX-1 in human stomach was similar to that in rat stomach suggests the possibility that PAR-1 in human stomach, as in rat stomach, may play a role in mucosal protection, although the possibility cannot completely be ruled out that the presence of PAR-1 in human but not rat platelets could lead to species differences in the role of PAR-1 in gastric mucosa. It is even likely that human platelet PAR-1, if activated locally in the gastric mucosa, might function to suppress or terminate the hemorrhage during gastric mucosal injury, which would contribute to mucosal protection.

Table 1 summarizes modulation of gastric functions by PAR-1 and PAR-2. PAR-1 activation mimics many of the gastric actions of PAR-2 activation, whereas the underlying mechanisms are not necessarily common. In conclusion, PAR-1 plays a protective role in gastric mucosa via endogenous prostanoid formation and modulates multiple gastric functions through prostanoid-dependent and -independent mechanisms.

References

1. Vu TK, Hung DT, Wheaton VI, Coughlin SR. Molecular cloning of a functional thrombin receptor reveals a novel proteolytic mechanism of receptor activation. Cell 1991;64:1057–1068.
2. Nystedt S, Emilsson K, Wahlestedt C, Sundelin J. Molecular cloning of a potential proteinase activated receptor. Proc Natl Acad Sci U S A 1994;91:9208–9212.

3. Kahn ML, Zheng YW, Huang W, Bigornia V, Zeng D, Moff S, Farese RV Jr, Tam C, Coughlin SR. A dual thrombin receptor system for platelet activation. Nature 1998;394:690–694.
4. Xu WF, Andersen H, Whitmore TE, Presnell SR, Yee DP, Ching A, Gilbert T, Davie EW, Foster DC. Cloning and characterization of human protease-activated receptor 4. Proc Natl Acad Sci U S A 1998;95:6642–6646.
5. Ishihara H, Connolly AJ, Zeng D, Kahn ML, Zheng YW, Timmons C, Tram T, Coughlin SR. Protease-activated receptor 3 is a second thrombin receptor in humans. Nature 1997;386:502–506.
6. Macfarlane SR, Seatter MJ, Kanke T, Hunter GD, Plevin R. Proteinase-activated receptors. Pharmacol Rev 2001;53:245–282.
7. Kawabata A. PAR-2: structure, function and relevance to human diseases of the gastric mucosa. Available at: http://www.expertreviews.org/02004799h.htm. Accessed July 7, 2002.
8. Nishikawa H, Kawabata A. Modulation of gastric functions by PARs. Drug Dev Res 2003;60:9–13.
9. Kawabata A, Nishikawa H, Kuroda R, Kawai K, Hollenberg MD. Proteinase-activated receptor-2 (PAR-2): regulation of salivary and pancreatic exocrine secretion in vivo in rats and mice. Br J Pharmacol 2000;129:1808–1814.
10. Kawabata A, Morimoto N, Nishikawa H, Kuroda R, Oda Y, Kakehi K. Activation of protease-activated receptor-2 (PAR-2) triggers mucin secretion in the rat sublingual gland. Biochem Biophys Res Commun 2000;270:298–302.
11. Kawabata A, Kuroda R, Morimoto N, Kawao N, Masuko T, Kakehi K, Kataoka K, Taneda M, Nishikawa H, Araki H. Lipopolysaccharide-induced subsensitivity of protease-activated receptor-2 in the mouse salivary glands in vivo. Naunyn Schmiedebergs Arch Pharmacol 2001;364:281–284.
12. Bohm SK, Kong W, Bromme D, Smeekens SP, Anderson DC, Connolly A, Kahn M, Nelken NA, Coughlin SR, Payan DG, Bunnett NW. Molecular cloning, expression and potential functions of the human proteinase-activated receptor-2. Biochem J 1996;314:1009–1016.
13. Nguyen TD, Moody MW, Steinhoff M, Okolo C, Koh DS, Bunnett NW. Trypsin activates pancreatic duct epithelial cell ion channels through proteinase-activated receptor-2. J Clin Invest 1999;103:261–269.
14. Saifeddine M, Al-Ani B, Cheng CH, Wang L, Hollenberg MD. Rat proteinase-activated receptor-2 (PAR-2): cDNA sequence and activity of receptor-derived peptides in gastric and vascular tissue. Br J Pharmacol 1996;118:521–530.
15. Corvera CU, Dery O, McConalogue K, Bohm SK, Khitin LM, Caughey GH, Payan DG, Bunnett NW. Mast cell tryptase regulates rat colonic myocytes through proteinase-activated receptor 2. J Clin Invest 1997;100:1383–1393.
16. Cocks TM, Sozzi V, Moffatt JD, Selemidis S. Protease-activated receptors mediate apamin-sensitive relaxation of mouse and guinea pig gastrointestinal smooth muscle. Gastroenterology 1999;116:586–592.
17. Kawabata A, Kuroda R, Nagata N, Kawao N, Masuko T, Nishikawa H, Kawai K. In vivo evidence that protease-activated receptors 1 and 2 modulate gastrointestinal transit in the mouse. Br J Pharmacol 2001;133:1213–1218.
18. Vergnolle N, Macnaughton WK, Al-Ani B, Saifeddine M, Wallace JL, Hollenberg MD. Proteinase-activated receptor 2 (PAR2)-activating peptides: identification of a receptor distinct from PAR2 that regulates intestinal transport. Proc Natl Acad Sci U S A 1998;95:7766–7771.
19. Kawabata A, Kinoshita M, Nishikawa H, Kuroda R, Nishida M, Araki H, Arizono N, Oda Y, Kakehi K. The protease-activated receptor-2 agonist induces gastric mucus secretion and mucosal cytoprotection. J Clin Invest 2001;107:1443–1450.
20. Hollenberg MD, Saifeddine M, Al-Ani B, Kawabata A. Proteinase-activated receptors: structural requirements for activity, receptor cross-reactivity, and receptor selectivity of receptor-activating peptides. Can J Physiol Pharmacol 1997;75:832–841.
21. Kawabata A, Kuroda R, Nishikawa H, Kawai K. Modulation by protease-activated receptors of the rat duodenal motility in vitro: possible mechanisms underlying the evoked contraction and relaxation. Br J Pharmacol 1999;128:865–872.
22. Buresi MC, Schleihauf E, Vergnolle N, Buret A, Wallace JL, Hollenberg MD, MacNaughton WK. Protease-activated receptor-1 stimulates $Ca^{(2+)}$-dependent $Cl^{(-)}$ secretion in human intestinal epithelial cells. Am J Physiol 2001;281:G323–G332.
23. Steinhoff M, Vergnolle N, Young SH, Tognetto M, Amadesi S, Ennes HS, Trevisani M, Hollenberg MD, Wallace JL, Caughey GH, Mitchell SE, Williams LM, Geppetti P, Mayer EA, Bunnett NW. Agonists of proteinase-activated receptor 2 induce inflammation by a neurogenic mechanism. Nat Med 2000;6:151–158.
24. Kawabata A, Kawao N, Kuroda R, Tanaka A, Itoh H, Nishikawa H. Peripheral PAR-2 triggers thermal hyperalgesia and nociceptive responses in rats. Neuroreport 2001;12:715–719.
25. Vergnolle N, Bunnett NW, Sharkey KA, Brussee V, Compton SJ, Grady EF, Cirino G, Gerard N, Basbaum AI, Andrade-Gordon P, Hollenberg MD, Wallace JL. Proteinase-activated receptor-2 and hyperalgesia: a novel pain pathway. Nat Med 2001;7:821–826.
26. Coelho AM, Vergnolle N, Guiard B, Fioramonti J, Bueno L. Proteinases and proteinase-activated receptor 2: a possible role to promote visceral hyperalgesia in rats. Gastroenterology 2002;122:1035–1047.
27. Hoogerwerf WA, Zou L, Shenoy M, Sun D, Micci MA, Lee-Hellmich H, Xiao SY, Winston JH, Pasricha PJ. The proteinase-activated receptor 2 is involved in nociception. J Neurosci 2001;21:9036–9042.
28. Nishikawa H, Kawai K, Nishimura S, Tanaka S, Araki H, Al-Ani B, Hollenberg MD, Kuroda R, Kawabata A. Suppression by protease-activated receptor-2 activation of gastric acid secretion in rats. Eur J Pharmacol 2002;447:87–90.
29. Kawao N, Sakaguchi Y, Tagome A, Kuroda R, Nishida S, Irimajiri K, Nishikawa H, Kawai K, Hollenberg MD, Kawabata A. Protease-activated receptor-2 (PAR-2) in the rat gastric mucosa: immunolocalization and facilitation of pepsin/pepsinogen secretion. Br J Pharmacol 2002;135:1292–1296.
30. Takeuchi K, Tanaka H, Furukawa O, Okabe S. Gastroduodenal HCO3-secretion in anesthetized rats: effects of 16,16-dimethyl PGE2, topical acid and acetazolamide. Jpn J Pharmacol 1986;41:87–99.
31. Naidu PS, Kulkarni SK. Possible involvement of prostaglandins in haloperidol-induced orofacial dyskinesia in rats. Eur J Pharmacol 2001;430:295–298.
32. Tanaka Y, Hayakawa S, Imai T, Akutsu A, Hirano H, Tanaka H, Nakahara T, Ishii K, Shigenobu K. Possible involvement of endothelium-derived hyperpolarizing factor (EDHF) in the depressor responses to platelet activating factor (PAF) in rats. Br J Pharmacol 2000;131:1113–1120.
33. McGuire JJ, Hollenberg MD, Andrade-Gordon P, Triggle CR. Multiple mechanisms of vascular smooth muscle relaxation by the activation of proteinase-activated receptor 2 in mouse mesenteric arterioles. Br J Pharmacol 2002;135:155–169.
34. Kawabata A, Kuroda R, Nishida M, Nagata N, Sakaguchi Y, Kawao N, Nishikawa H, Arizono N, Kawai K. Protease-activated receptor-2 (PAR-2) in the pancreas and parotid gland: Immunolocalization and involvement of nitric oxide in the evoked amylase secretion. Life Sci 2002;71:2435–2446.
35. Asfaha S, Brussee V, Chapman K, Zochodne DW, Vergnolle N. Proteinase-activated receptor-1 agonists attenuate nociception in response to noxious stimuli. Br J Pharmacol 2002;135:1101–1106.
36. Kawabata A, Kawao N, Kuroda R, Tanaka A, Shimada C. The PAR-1-activating peptide attenuates carrageenan-induced hyperalgesia in rats. Peptides 2002;23:1181–1183.

37. Hollenberg MD, Laniyonu AA, Saifeddine M, Moore GJ. Role of the amino- and carboxyl-terminal domains of thrombin receptor-derived polypeptides in biological activity in vascular endothelium and gastric smooth muscle: evidence for receptor subtypes. Mol Pharmacol 1993;43:921–930.
38. Edwards G, Weston AH. EDHF—are there gaps in the pathway? J Physiol 2001;531:299.
39. Hollenberg MD, Yang SG, Laniyonu AA, Moore GJ, Saifeddine M. Action of thrombin receptor polypeptide in gastric smooth muscle: identification of a core pentapeptide retaining full thrombin-mimetic intrinsic activity. Mol Pharmacol 1992;42:186–191.

Received August 28, 2003. Accepted October 9, 2003.

Address requests for reprints to: Atsufumi Kawabata, Ph.D., Division of Physiology and Pathophysiology, School of Pharmaceutical Sciences, Kinki University, 3-4-1 Kowakae, Higashi-Osaka 577-8502, Japan. e-mail: kawabata@phar.kindai.ac.jp; fax: (81) 6-6730-1394.

Supported in part by a Grant-in-Aid for Scientific Research from the Japan Society of the Promotion of Science.

MINIREVIEW

Trends in Glycoscience and Glycotechnology
Vol.17 No.97 (September 2005) pp.193–203

Mass Spectrometry of Glycoproteins

糖タンパク質の質量分析

Kawasaki, Nana[*1,2]; Itoh, Satsuki[1]; Harazono, Akira[1]; Hashii, Noritaka[1,2]; Matsuishi, Yukari[1,2]
Hayakawa, Takao[3]; and Kawanishi, Toru[1]

[1]Division of Biological Chemistry and Biologicals, National Institute of Health Science,
1-18-1, Kamiyoga, Setagaya-ku, Tokyo, 158-8501, Japan
[2] Core Research for Evolutional Science and Technology (CREST) of Japan Science and Technology Agency (JST),
Kawaguchi Center Building, 4-1-8, Hon-cho, Kawaguchi, Saitama 332-0012, Japan
[3] Pharmaceutical and Medical Devices Agency, 3-3-2 Kasumigaseki, Chiyoda-ku, Tokyo, 100-0013, Japan
[*]Correspondence to: Nana Kawasaki, National Institute of Health Sciences,
Division of Biological Chemistry and Biologicals, 1-18-1 Kamiyoga, Setagaya-ku, Tokyo, 158-8501, Japan
FAX: 81-3-3700-9084, E-mail: nana@nihs.go.jp

Key Words: *MS, MS/MS, MS^n, glycoprotein, oligosaccharide, glycopeptide*

Abstract

This review presents mass spectrometric methods for glycoprotein identification, determination of glycosylation sites, structural elucidation of carbohydrates, and their applications to glycomics and proteomics.

要　約

本レビューでは、質量分析を用いた糖タンパク質同定、糖鎖結合位置の決定、糖鎖構造解析、及びグライコミクス・プロテオミクスへの応用について紹介する。

A. Introduction

Mass spectrometry (MS) has become a powerful tool for glycoprotein identification, and the determination of glycosylation sites, and structural features of carbohydrates, such as sequence, linkage and branching at each glycosylation site. Generally, the mass spectrometric characterization of glycoprotein involves the following steps: 1) fractionation of enzymatically or chemically liberated glycans followed by MS, and 2) fractionation of glycopeptides from proteolytic digests followed by MS. Here we present the MS of glycan and glycopeptides using the latest applications.

B. MS of Liberated Glycans

Matrix-assisted laser desorption/ ionization (MALDI) (1), and electrospray ionization (ESI) (2), which are soft ionization techniques, are often used for glycan molecular mass determination. MALDI has been used by preference for rapid microanalyses, however, it generates metastable ions and the consequent various fragmentations, including the depletion of terminal sialic acids (known as post-source decay, PSD) (3). Although ESI used to have a problem with sensitivity, the introduction of nanospray technology allows us to use ESI to analyze femtomole levels of glycans (4). To measure all types of glycans, including neutral glycans and sulfated or sialylated acidic glycans, we suggest mass spectrometric glycan analysis in both positive and negative ion modes.

MALDI and ESI are combined with several types of

A. 緒　言

質量分析 (MS) は、糖タンパク質の同定、糖鎖結合位置の決定、並びに各結合位置における糖鎖の配列、結合位置、及び分岐等を含む構造特性解析の有用な手段として利用されている。現在、MS を用いた糖鎖解析のアプローチとしては、1) 酵素的または化学的に切り出された糖鎖の分画と MS、及び 2) 糖タンパク質酵素消化物からの糖ペプチドの分画と MS、が一般的である。そこで、ここでは、遊離糖鎖と糖ペプチドの MS について、最近の分析例を取り上げながら解説する。

B. 遊離糖鎖の MS

糖鎖分子の分析に適したソフトイオン化法として、マトリクス支援レーザー脱離イオン化法 (MALDI) (1)、及びエレクトロスプレーイオン化法 (ESI) (2) がよく利用されている. MALDI は迅速分析及び微量分析に適しているが、準安定イオンが生成し、MS^1 スペクトル上にはシアル酸が脱離したイオンをはじめとする様々なフラグメントが検出される (ポストソース分解、PSD) (3)。ESI は感度上の問題が指摘されてきたが、現在ではナノスプレーの開発によって、フェムトモルレベルの糖鎖分析が可能となっている (4)。糖鎖には中性糖鎖だけでなく、シアル酸や硫酸基などが結合した酸性糖鎖が存在するので、未知試料を分析する際には、ポジティブ及びネガティブ両イオンモードで測定するのが望ましい。

MALDI や ESI は様々なアナライザー (分析計) と組み合

analyzer, such as quadrupole (Q) (5), quadrupole ion trap (IT) (6), time-of-flight (TOF) (7), and Fourier transform ion cyclotron resonance (FTICR) (8). Tandem mass spectrometers with various combinations of these analyzers have recently become available. Tandem mass spectrometry (MS/MS) is widely recognized as an effective means of structural elucidation, including molecular mass measurement by MS^1 and oligosaccharide sequencing by collision-induced dissociation (CID)-MS/MS (9–11). In particular, ITMS instruments are becoming popular for multistage tandem mass spectrometry (MS^n), which offers multiple precursor selections and CID experiments (12, 13).

Fig. 1A shows types of carbohydrate fragmentation by CID-MS/MS (14). In the positive ion mode the most common fragmentation involves cleavage of the glycosidic bond with retention of the glycosidic oxygen atom by species formed from the reducing end (Fig. 1B). Fragment ions generated by this cleavage are represented as B-ion (non-reducing end) and Y-ion (reducing end). The cleavage of carbon-carbon bonds of the sugar ring yields A-ion and X-ion. These cross ring fragments are often used as decisive ions in linkage determination (15, 16).

Fig. 2 shows the positive ion ESI-MS/MS and MS^3 spectra of pyridylaminated agalacto-triantennary oligosaccharide (I) (Figs. 2A, A') and bisected agalacto-biantennary oligosaccharide (II) (Figs. 2B, B'). These are positional isomers whose one GlcNAc is attached to either α1-3/6 Man or β1-4Man in the trimannosyl core and cannot

わせて利用されている。アナライザーには四重極型 (Q) (5)、イオントラップ型 (IT) (6)、飛行時間型 (TOF) (7)、及びフーリエ変換イオンサイクロトロン共鳴型 (FTICR) (8) MS 装置などが用いられている．現在では、これらの分析装置を様々に組み合わせたタンデム質量分析装置の利用が可能である。タンデム質量分析 (MS/MS) は、MS^1 による糖鎖の質量測定と、衝突誘起解離 (CID)-MS/MS による糖鎖の配列解析を同時に行うことができる (9–11)。特に ITMS 装置は、前駆イオンの選択と CID-MS/MS を繰り返す多段階 MS/MS (MS^n) が可能であることから、近年、糖鎖解析用装置としての人気が高い (12、13)。

図 1A は、CID-MS/MS における糖鎖の開裂を示したものである (14)。ポジティブイオンモードで測定した糖鎖の CID-MS/MS では主に、グリコシド結合の酸素原子を還元末端側糖鎖に残した開裂が生じる (図 1B). そのとき生じた非還元末端側イオンは B イオン、還元末端側イオンは Y イオンと呼ばれ、糖鎖の配列解析に利用される。ピラノース環の炭素 - 炭素間の結合が開裂して生じたイオンは A、及び X イオンと呼ばれ、糖鎖結合位置の決め手となることがある (15、16)。

図 2 は、ピリジルアミノ化されたアガラクト 3 本鎖糖鎖 (I) 及びアガラクトバイセクト 2 本鎖糖鎖 (II) のポジティブイオン MS/MS (図 2A、B)、及び MS^3 (図 2A'、B') スペクトルである。これらの糖鎖は GlcNAc 1 分子がトリマンノシルコアの α1-3/6Man または β1-4Man に結合した位置異性体で、MS^1 による分子量測定では区別することはできない。しかし、MS^n によっ

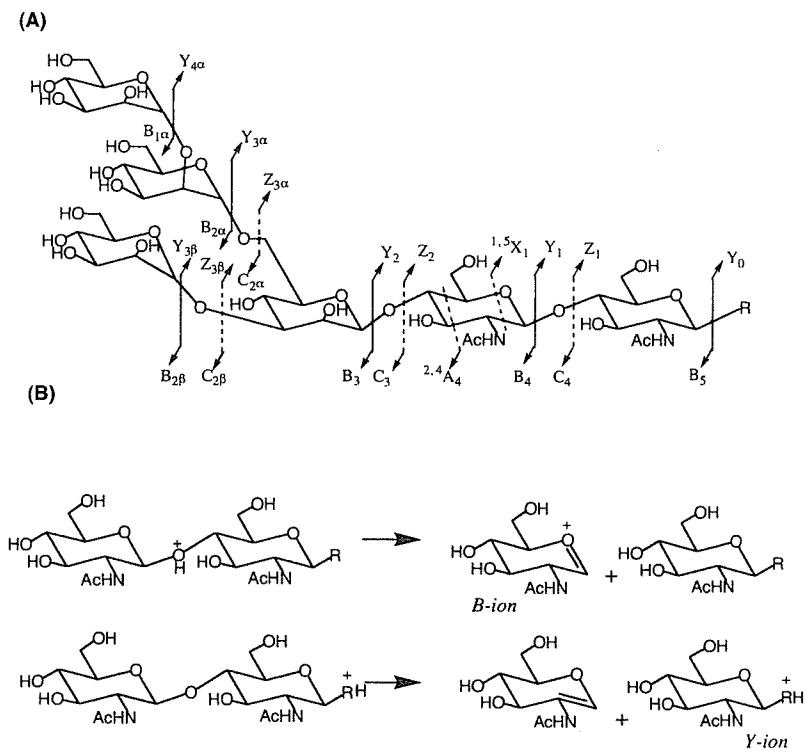

Fig. 1. (A) Types of carbohydrate fragmentation. (B) Production of B- and Y-ions in the positive ion mode.

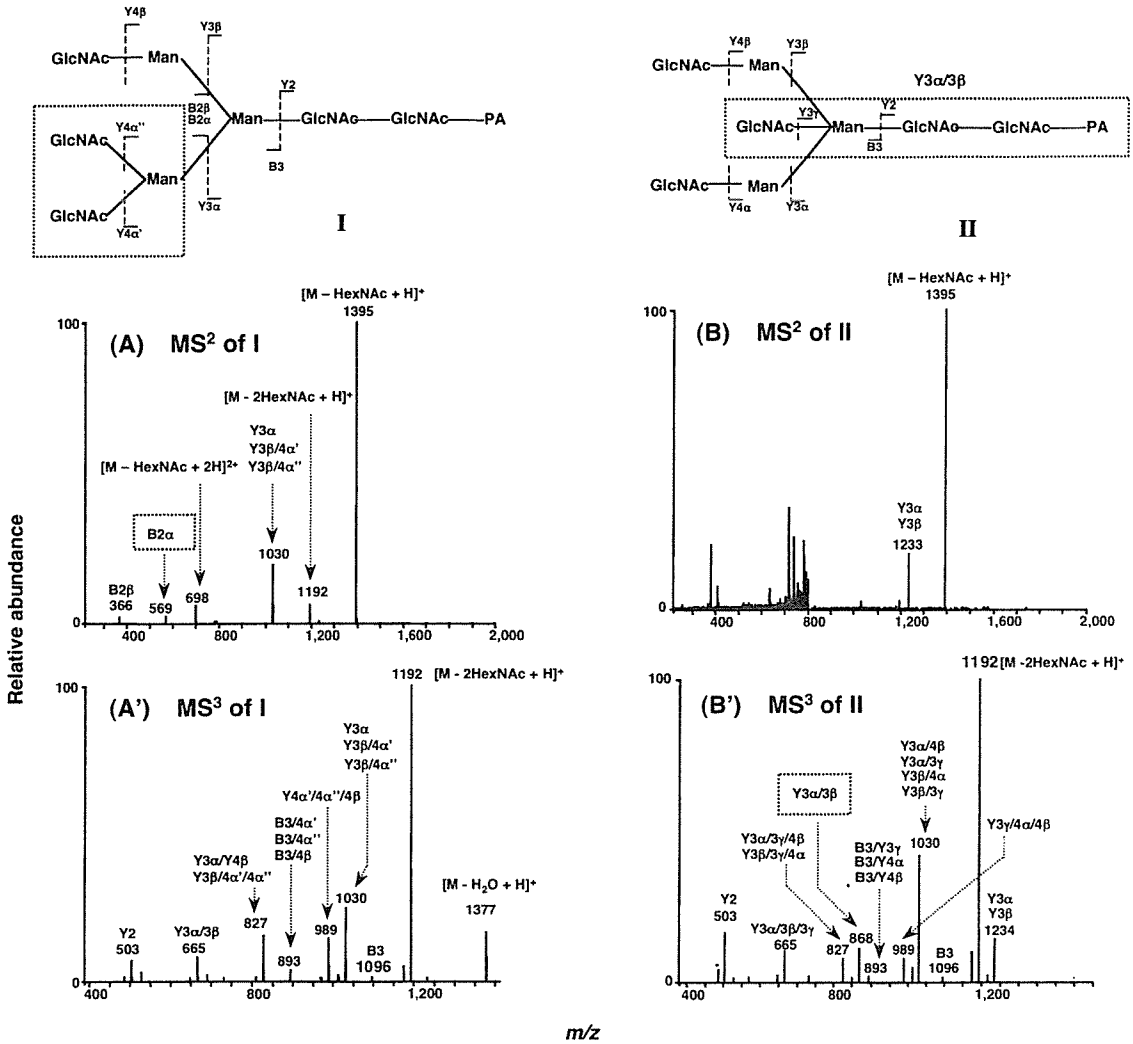

Fig. 2. MS^n spectra of oligosaccharides. (A) MS/MS spectrum of oligosaccharide I (precursor ion: *m/z* 800.8). (A') MS^3 spectrum of oligosaccharide I (precursor ion: *m/z* 1,395.4). (B) MS/MS spectrum of oligosaccharide II (precursor ion: *m/z* 800.5). (B') MS^3 spectrum of oligosaccharide II (precursor ion: *m/z* 1,395.4). MS: LTQ (Thermo Electron).

be discriminated by MS^1 (molecular mass determination). In contrast, MS^n spectra clearly show structural differences between two glycans. B-ion corresponding to $GlcNAc_2Man^+$ is observed at *m/z* 569 in the MS/MS spectrum of glycan I (Fig. 2A), while Y-ion at *m/z* 868 corresponding to [GlcNAc-Man-GlcNAc-GlcNAc-PA + H]$^+$ is detected in MS^3 spectrum of glycan II (Fig. 2B'). In particular, glycan II can be determined as bisected oligosaccharides on the basis of a bisected *N*-glycan diagnostic ion at *m/z* 868.

The MS^n spectra of some glycans exhibit characteristic fragment patterns. Hence, even if no diagnostic ion, such as a bisected glycan-specific fragment, is detected, the glycan structure can be sometimes deduced from ion intensity ratios obtained by MS^n (17,18). For instance, structures of branched arms were deduced from mass spectrometric patterns obtained by MS/MS which causes a cleavage of α1-3 linkage more than α1-6 linkage (19–21). However, complete structural

て両者の構造の違いを明確にすることができる。例えば、糖鎖 I の MS/MS スペクトルには *m/z* 569 に $GlcNAc_2Man^+$ に相当する B イオンが検出され（図 2A）、糖鎖 II の MS^3 スペクトル（前駆イオン：*m/z* 1395 [M-HexNAc + H]$^+$）には [GlcNAc-Man-GlcNAc-GlcNAc-PA + H]$^+$ に相当するイオンが *m/z* 868 に検出されている（図 2B'）。特に、[GlcNAc-Man-GlcNAc-GlcNAc-PA + H]$^+$ (*m/z* 868) はバイセクト糖鎖に特異的なフラグメントであり、糖鎖 II がバイセクト糖鎖であることを決定づけている。

糖鎖の MS^n は特徴的なスペクトルパターンを示すことが多いので、構造特異的イオンが検出されない場合でも、MS^n スペクトルのパターンより糖鎖構造を推定できる場合がある (17,18)。例えば、トリマンノシルコアの α1-3 結合が α1-6 結合よりも開裂しやすいことを利用して、分岐構造を解析した例が報告されている (19–21)。しかし、MS 単独で糖鎖構造を完

elucidation by MS alone is still a great challenge, and additional experiments are required, such as exoglycosidase digestion (22), lectin affinity chromatography (23), and sugar mapping (17,24,25).

C. Glycan Profiling by LC/MS

Many different oligosaccharides are attached to a glycoprotein. The development of derivatization and separation techniques for glycans has been an important part of structural glycobiology (26–34). The derivatization of glycan with a hydrophobic molecule improves the ionization efficiency of hydrophilic glycans and offers higher sensitivity (31,35). A combination of various HPLC techniques with off-line MALDI-MS or on-line ESI-MS has been successful in oligosaccharide profiling as well as the elucidation of structural details (36–39). As an example, we present the mass spectrometric *N*-glycan profiling of CHO cells and cells transfected with *N*-acetylglucosaminyltransferase III, which catalyzes the addition of GlcNAc to β1-4Man in the trimannosyl core (Fig. 3) (40). Mass spectrometric analysis reveals the difference in glycosylation between two samples and the appearance of peaks with additional HexNAc (203 Da) in the transfected cells.

We recently demonstrated quantitative oligosaccharide

全に同定することが困難である場合が多く、MS はエキソグリコシダーゼによる段階的消化法 (22)、レクチンアフィニティークロマトグラフィー (23)、及び糖鎖マッピング (17、24、25) などと組み合わせて用いられることが多い。

C. LC/MS を用いた糖鎖プロファイリング

糖タンパク質には様々な糖鎖が結合しているので、糖鎖の標識法と分離技術の開発は、構造糖鎖生物学において重要な位置を占めている (26–34)。糖鎖を分離・検出するために開発された疎水性物質による誘導体化は、親水性の高い糖鎖のイオン化効率を向上させるので、MS における高感度化においても有用である (31、35)。さらに、様々な HPLC による分離法とオフライン MALDI-MS、あるいはオンライン ESI-MS を組み合わせた分析方法は、糖鎖プロファイリングと糖鎖構造解析を兼ね備えた方法として利用され、多くの成果を上げている (36–39)。一例として図 3 に CHO 細胞、及びトリマンノシルコアの β1-4Man に GlcNAc を付加させる *N*- アセチルグルコサミン転移酵素 III (GnT-III) 遺伝子を導入した CHO 細胞の MS を用いた糖鎖プロファイリングの結果を示す (40)。MS を利用することによって、GnT-III 導入細胞で新たに出現した糖鎖は、HexNAc1 分子 (203Da) 増加した糖鎖であることが確認できる。

筆者らは最近、安定同位体標識化 2- アミノピリジン (AP) を用いた標識法と LC/MS を組み合わせた定量的糖鎖プロファ

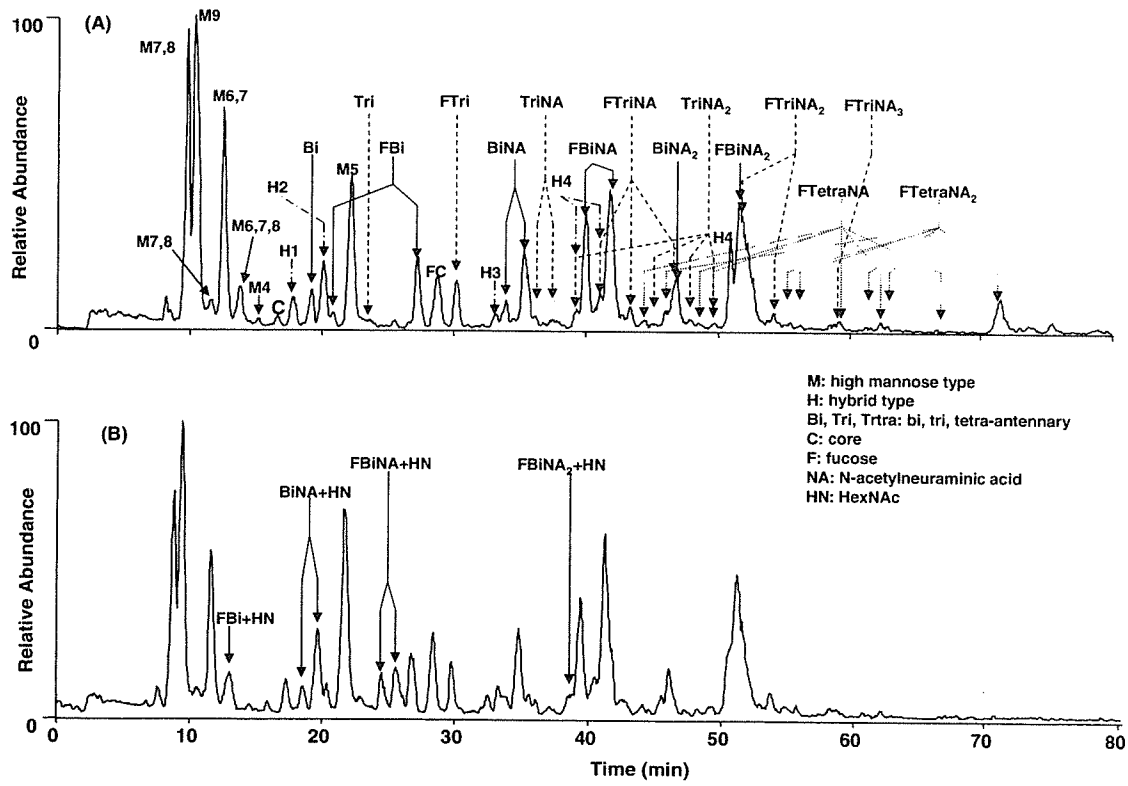

Fig. 3. TICs of *N*-linked oligosaccharides released from the insoluble fractions. (A) CHO cells. (B) *N*-acetyl glucosaminyltransferase III-transfected CHO cells. Column: Hypercarb (0.2 x 150 mm, Thermo Electron), LC: Magic 2002 (Michrome BioResources), MS: TSQ-7000 (Thermo Electron), Eluent: 5 mM ammonium acetate containing acetonitrile.